

Supplementary Materials for

Multiplicity conversion based on intramolecular triplet-to-singlet energy transfer

A. Cravcenco, M. Hertzog, C. Ye, M. N. Iqbal, U. Mueller, L. Eriksson, K. Börjesson*

*Corresponding author. Email: karl.borjesson@gu.se

Published 20 September 2019, *Sci. Adv.* **5**, eaaw5978 (2019)

DOI: 10.1126/sciadv.aaw5978

This PDF file includes:

Section S1. Synthesis and characterization

Section S2. Details of the experimental determination of the rate of energy transfer

Section S3. Details of the simulation of the rate of energy transfer

Section S4. X-ray diffraction of **19** and DBA

Scheme S1. Synthesis of the DBA.

Table S1. Excited-state lifetimes (fractional contributions in parentheses) and associated emission quantum yields for D, A, and DBA in toluene solutions.

Fig. S1. Emission quantum yield of A, measured using an integrated sphere.

Fig. S2. Transient absorption spectroscopy and decay of D in toluene when excited at 320 nm.

Fig. S3. Transient absorption spectroscopy of DBA in toluene solution when excited at 320 nm.

Fig. S4. Transient absorption decays of DBA when excited at 320 nm.

Fig. S5. The simulated rate of energy transfer as a function of dihedral angle (orange line).

Fig. S6. Lifetime of DBA with different excitation intensity.

Fig. S7. Structure of the ligand (**19**), as solved by x-ray diffraction.

Fig. S8. Structure of DBA (**20**), as solved by x-ray diffraction.

Fig. S9. ¹H NMR (400 MHz, CDCl₃), **6**.

Fig. S10. ¹³C NMR (101 MHz, CDCl₃), **6**.

Fig. S11. ¹H NMR (800 MHz, CDCl₃), **15**.

Fig. S12. ¹³C NMR (201 MHz, CDCl₃), **15**.

Fig. S13. ³¹P NMR (162 MHz, CDCl₃), **15**.

Fig. S14. ¹H NMR (800 MHz, CDCl₃), **17**.

Fig. S15. ¹³C NMR (201 MHz, CDCl₃), **17**.

Fig. S16. ¹H NMR (800 MHz, DMSO-d₆), **18**.

Fig. S17. ¹³C NMR (201 MHz, DMSO-d₆), **18**.

Fig. S18. ¹H NMR (800 MHz, DMSO-d₆), **19**.

Fig. S19. ¹³C NMR (201 MHz, DMSO-d₆), **19**.

Fig. S20. ¹H NMR (800 MHz, CDCl₃), **20**.

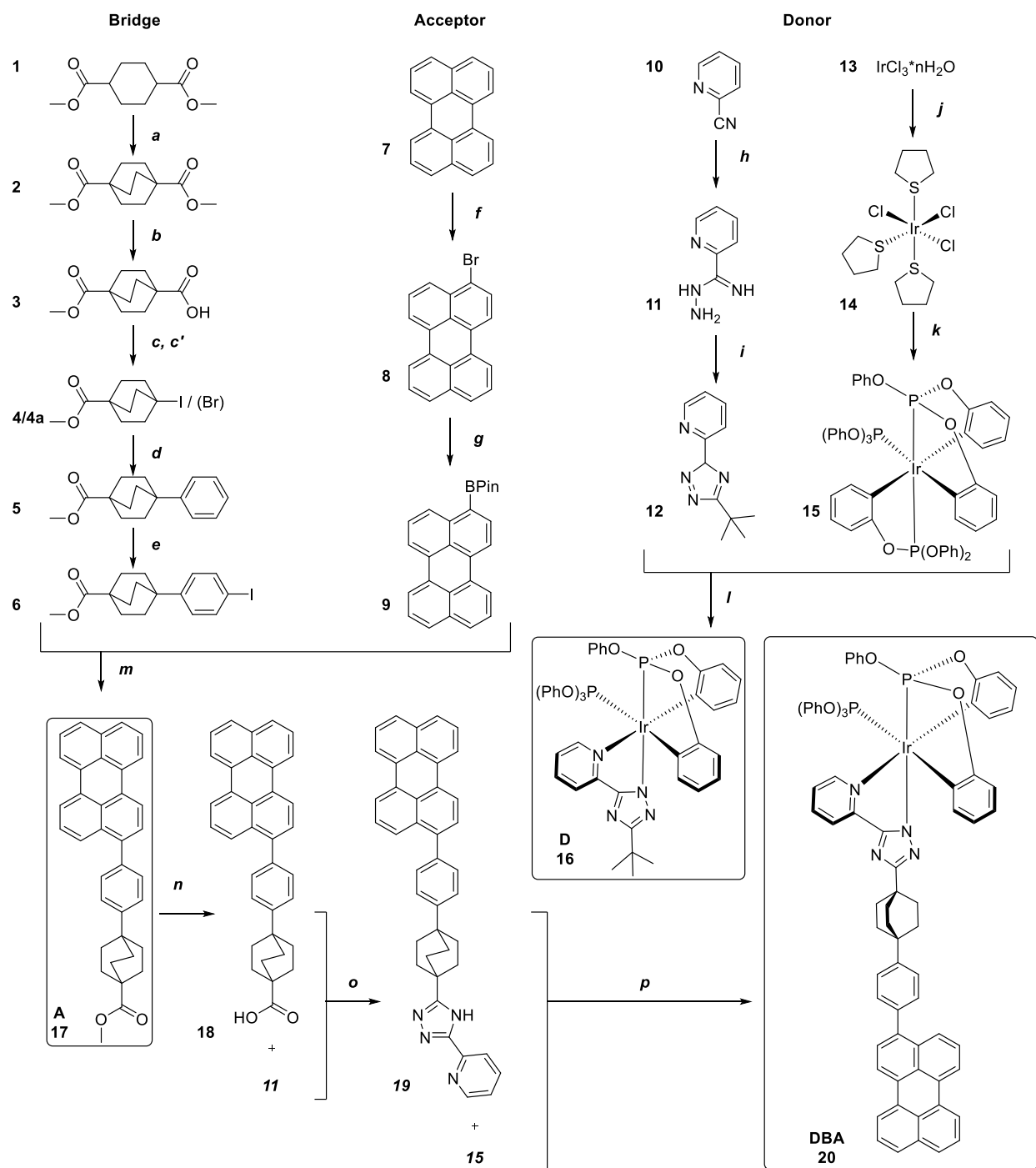
Fig. S21. ¹³C NMR (201 MHz, CDCl₃), **20**.

Fig. S22. ³¹P NMR (162 MHz, CDCl₃), **20**.

Fig. S23. HRMS (ESI+), **6**.
Fig. S24. HRMS (ESI+), **15**.
Fig. S25. HRMS (ESI+), **17**.
Fig. S26. HRMS (ESI+), **18**.
Fig. S27. HRMS (ESI+), **19**.
Fig. S28. HRMS (ESI+), **20**.
References (26–47)

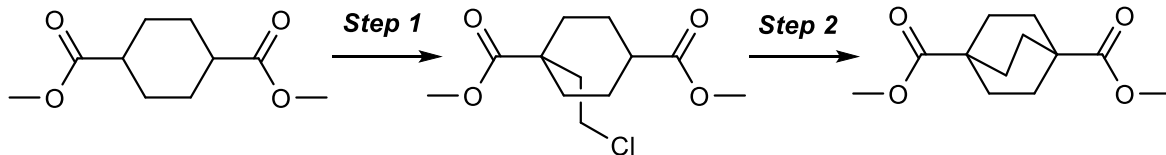
Section S1. Synthesis and characterization

A convergent synthetic strategy was applied for the synthesis of the donor-bridge-acceptor dyad (Scheme 1). Since the most important spectral feature of the dyad components is a considerable overlap between the donor emission and acceptor absorption, both functional components were selected with great accuracy. As a donor (D) an Ir^{III} complex bearing tripodal, facially coordinated phosphite and 2-pyridyltriazolate ligand was chosen (**16**). This photostable iridium complex has been shown to exhibit blue phosphorescence and been used in state-of-the-art OLEDs that possess deep-blue chromaticity (24). Taking into consideration the emission spectrum of the donor (**16**), perylene was selected as a suitable acceptor (A, **17**) counterpart. Perylene is a well-studied chromophore with a fluorescence quantum yield close to unity and a small Stokes shift (25). The bridging unit has a pivotal importance in spatially separating the donor and the acceptor moieties. The rigid structure of bicyclo[2.2.2]octane permits free rotation only along the long axis of the molecule offering a stable position for the functional counterparts of the dyad (DBA, **20**). The synthesis of the donor (D, **16**) followed a modified literature procedure (24), where implementation of microwave-assisted complexation significantly reduced the reaction time. In addition, intermediate complex (**15**) was for the first time isolated and characterized. To synthesize the bridging unit, diester was prepared by a two-step sequence reported by Chang et al., (26) followed by a selective monohydrolysis to provide the acid (**3**). Two alternative pathways were used for halodecarboxylation: a classical Hunsdiecker-Borodin protocol (27), and a more modern approach using photoredox halodecarboxylation (28). Both strategies afforded the target halides (**4**, **4a**) in high yields. Thus, the photoredox procedure offers an environmentally friendly alternative to traditional Hunsdiecker-Borodin, which relies on mercury or silver salts. Cross-coupling of inactivated tertiary alkyl halides to aromatic compounds represents a huge challenge in modern synthetic chemistry and reports on such transformations are rather scarce. All attempts to install (**4**) at the ortho position of the perylene were unsuccessful. Therefore, a phenyl spacer was introduced in between the perylene unit and the bicyclo[2.2.2]octane bridge. Friedel-Crafts alkylation of benzene (29) allowed access to methyl ester (**5**) in close to quantitative yields, followed by selective halogenation giving the iodoester (**6**) (30). To couple the acceptor to the bridging unit, perylene was brominated at the ortho position using stoichiometric amounts of NBS (31-33). Borylation afforded the pinacol ester (**9**) (34) that was coupled to the bridge by a Suzuki cross coupling affording the desired perylene containing fragment (**17**), which was used as acceptor (A) unit in the photophysical experiments. To complete the acceptor containing ligand (**14**), the ester (**17**) was hydrolysed (35) and converted to the corresponding acid chloride, which was heated together with hydrazonamide (**11**) to perform an intramolecular cyclization giving (**14**). The triazole containing ligand (**14**) was coordinated to iridium complex (**15**) yielding the final donor-bridge-acceptor dyad (DBA, **20**), as confirmed by single crystal X-ray.



Scheme S1. Synthesis of the DBA. Synthesis of the donor-bridge-acceptor (DBA) dyad. Reaction conditions: *a*) LDA (2 M), Br(CH₂)₂Cl, DMPU/THF, -78 °C, 12 h; then LDA (2 M), DMPU/THF, -78 °C, 12 h; *b*) KOH, MeOH, reflux, 5 h; *c*) H₂O, I₂, CHCl₃, reflux, 6 h; *c'*) Ir(PC), Cs₂CO₃, diethyl bromomalonate, hv (455 nm), PhCl, 4 h; *d*) AlCl₃, PhH, 12 h; *e*) (CF₃COO)₂IPh, I₂, CHCl₃, 1 h; *f*) NBS, THF, 24 h; *g*) B₂(pin)₂, Pd(dppf)Cl₂, KOAc, 1,4-dioxane, 80 °C 24 h; *h*) (NH₂)₂, EtOH, 12h; *i*) Me₃CCOCl, Na₂CO₃, DMAA/THF, 4 h; then ethylene glycol, 190 °C, 1 h; *j*) tetrahydrothiophene, 2-MeOEtOH, 130 °C, 6 h; *k*) P(OPh)₃, NaOAc, Decalin/ODCB, MW 190 °C, 1h; *m*) Pd(Ph₃P)₄, K₂CO₃ (2 M), Aliquat 336 (cat.), 80 °C, 24 h; *n*) KOH, THF/H₂O, reflux, 48 h; *o*) (COCl)₂, DMF (cat.), 1 h; then **11**, Na₂CO₃, DMAA/THF, 4 h; then ethylene glycol, 190 °C, 1 h; *p*) NaOAc, Ir[P(OPh)₃](tpit)₂, Decalin/ODCB, MW 190 °C, 6h.

a) dimethyl bicyclo[2.2.2]octane-1,4-dicarboxylate (2)



Step 1:

To a stirred solution of 2M LDA (13.5 mL, 27.5 mmol) in THF (20 mL), cooled to $-78\text{ }^{\circ}\text{C}$, was added DMPU (12 mL, 100 mmol). Thereafter, a solution of dimethyl cyclohexane-1,4-dicarboxylate (5.0 g, 25 mmol) in anhydrous THF (5 mL) was slowly added over 30 min. The mixture was stirred for an additional 40 min at $-78\text{ }^{\circ}\text{C}$ and 1-bromo-2-chloroethane (2 mL, 25 mmol) was added dropwise and stirred for an additional 60 min at $-78\text{ }^{\circ}\text{C}$. The cooling bath was removed, and the mixture was allowed to reach ambient temperature. The reaction was quenched with saturated aqueous NH_4Cl (40 mL) and extracted with CH_2Cl_2 (2 x 150 mL). The organic phase was dried with Na_2SO_4 and concentrated under reduced pressure. The concentrate passed through a plug of silica gel washing with CH_2Cl_2 (50 mL) and solvent was removed under reduced pressure. Crude material was used for second step without any purification.

Step 2:

To a stirred solution of 2M LDA (13.5 mL, 27.5 mmol) in THF (20 mL), cooled to $-78\text{ }^{\circ}\text{C}$, DMPU (12 mL, 100 mmol) was added. A solution of dimethyl 1-(2-chloroethyl)cyclohexane-1,4-dicarboxylate (6.5 g, 25 mmol) in anhydrous THF (5 mL) was slowly added over 30 min. The reaction mixture was stirred at $-78\text{ }^{\circ}\text{C}$ for 1 h. The cooling bath was removed, and the mixture was allowed to reach ambient temperature. The clear brown reaction mixture was then quenched with saturated aqueous NH_4Cl (40 mL) and extracted with CH_2Cl_2 (2 x 150 mL). The organic phase was dried with Na_2SO_4 and concentrated *in vacuo*. The crude product was subjected to flash column chromatography (gradient elution of hexanes \rightarrow 20% EtOAc/hexanes) to give (3.67 g, 65%) of desired product in form of white crystals. Spectroscopic properties were in agreement with literature values (26).

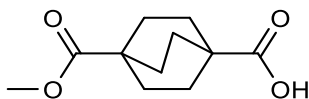
^1H NMR (400 MHz, CDCl_3): δ = 3.61 (s, 3H), 1.75 (s, 6H).

^{13}C NMR (101 MHz, CDCl_3): δ = 177.72, 51.65, 38.56, 27.68.

GC-MS (ESI+): m/z ($\text{M}+\text{H}$) $^+$ = 226.

m.p. = $92\text{--}94\text{ }^{\circ}\text{C}$.

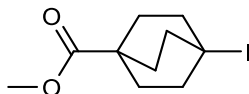
b) 4-(methoxycarbonyl)bicyclo[2.2.2]octane-1-carboxylic acid (3)



Potassium hydroxide (1.16 g, 20 mmol) was added portion wise to a stirred solution of **2** (3.67 g, 17.3 mmol) in MeOH (30 mL) and resulting mixture heated to reflux point for 5h. The flask was removed from heating bath and allowed to cool down to room temperature. The volatiles were removed by rotary evaporation, where after residue was acidified to pH~3 and extracted with CH_2Cl_2 (2 x 100 mL). The organic phase was dried over Na_2SO_4 and concentrated under reduced pressure to give the desired product as a white solid (2.2 g, 60%). NMR Chemical shifts were in line with those published (36).

^1H NMR (400 MHz, CDCl_3): δ = 1.96 (s, 3H), 2.07 (s, 12H).
 ^{13}C NMR (101 MHz, CDCl_3): δ = 27.6, 27.7, 38.5, 38.7, 51.8, 177.8, 183.4.
GC-MS (ESI+): m/z ($\text{M}+\text{H}$) $^+$ = 212.
m.p. = 172-173 °C.

c) methyl 4-iodobicyclo[2.2.2]octane-1-carboxylate (**4**)



Compound **3** (1.0 g, 4.71 mmol) was dissolved in CH_2Cl_2 (20 mL), where after HgO (1.53 g, 7.81 mmol) and Iodine (2.4 g, 9.43 mmol) were added. The reaction mixture was then heated in a sealed microwave vial to 80-90 °C overnight. The heating bath was removed and the mixture was allowed to reach ambient temperature. Saturated aqueous sodium thiosulfate (2×40 mL) was added and reaction mixture extracted with CH_2Cl_2 (2×100 mL). The organic phase was dried over Na_2SO_4 and passed through a short plug of silica gel washing with 20 mL. Volatiles were removed *in vacuo* to yield the title product (0.96 g, 70%) as colorless crystals. Spectroscopic data was in accordance with literature values (27, 37).

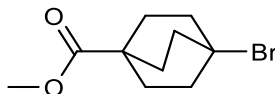
^1H NMR (400 MHz, CDCl_3): δ = 1.23 (t, J = 7 Hz, 3H), 1.88-2.00 (m, 6H), 2.41-2.54 (m, 6H), 4.09 (q, J = 7 Hz, 2H).

^{13}C NMR (101MHz, CDCl_3): δ = 177.20, 51.77, 42.92, 39.80, 31.80, 35.57.

GC-MS (ESI+): m/z ($\text{M}+\text{H}-\text{I}$) $^+$ = 167.

m.p. = 106-107 °C.

c') methyl 4-bromobicyclo[2.2.2]octane-1-carboxylate (**4a**)



Compound **4a** was synthesized by photoredox halodecarboxylation using synthetic methodology reported by F. Glorius et al.(28) Compound **3** (300 mg, 1.41 mmol) was placed in a microwave vial containing cesium carbonate (460.5 mg, 1.41 mmol), $(\text{Ir}[\text{dF}(\text{CF}_3)\text{ppy}]_2(\text{dtbpy}))\text{BF}_4^*$ (29 mg, 0.0282 mmol, 2mol%) and chlorobenzene (18 mL). Microwave vial was sealed with a Teflon liner cap and diethyl bromomalonate (652 μL , 3.525 mmol) was added via syringe.

Reaction mixture was sparged with argon for 30 min and then stirred for 4 h hours under blue LED (455 nm) irradiation. Contents were filtered through a short plug of silica gel washing with CH_2Cl_2 (10 mL) and solvents evaporated under reduced pressure. Silica gel flash chromatography (gradient of hexanes \rightarrow 10% EtOAc/hexanes) afforded (227 mg, 65%) of title compound as colorless crystals. NMR Chemical shifts were in line with those published (29).

^1H NMR (400 MHz, CDCl_3): δ = 1.94-1.98 (m, 6H), 2.23-2.27 (m, 6H), 3.64 (s, 3H).

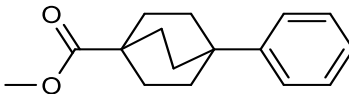
^{13}C NMR (101 MHz, CDCl_3): δ = 177.09, 62.12, 51.86, 36.85, 31.14.

GC-MS (ESI+): m/z ($\text{M}-\text{Br}+\text{H}$) $^+$ = 167.

m.p.= 264-267 °C.

* - Same catalyst bearing PF_6 counterion is commercially available on Sigma-Aldrich.

d) methyl 4-phenylbicyclo[2.2.2]octane-1-carboxylate (5)



To a suspension of AlCl₃ (809 mg, 6.07 mmol) in benzene (4 mL, 1.21 mmol) at -10 °C under nitrogen atmosphere, was added a solution of **4a** (300 mg, 1.214 mmol) in benzene (2 mL). The reaction mixture was gradually warmed up to room temperature and stirred overnight. It was carefully poured into ice water and extracted with EtOAc (2 x 50 mL). The combined organic layers were washed with brine, dried over Na₂SO₄, and filtered. Solvents were removed by rotary evaporation and crude material purified by silica gel flash chromatography (gradient hexanes → 20% EtOAc/hexanes) to afford title compound (250 mg, 84%) as a tan solid. Spectroscopic values were in line with those previously published (29).

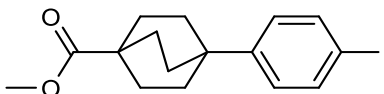
¹H NMR (400 MHz, CDCl₃): δ = 7.36-7.29 (m, 4H), 7.20-7.16 (m, 1H), 3.67 (s, 3H), 1.98-1.80 (m, 12 H).

¹³C NMR (101 MHz, CDCl₃): δ = 178.43, 149.10, 128.11, 125.71, 125.44, 51.68, 39.07, 34.59, 31.68, 31.67, 28.76.

GC-MS (ESI): *m/z* (M+H)⁺ = 244.

m.p. = 84-86 °C.

e) methyl 4-(4-iodophenyl)bicyclo[2.2.2]octane-1-carboxylate (6)



Compound **6** was prepared according to the literature procedure (30).

[Bis(trifluoroacetoxy)iodo]benzene (1.44 g, 3.35 mmol) and Iodine (0.4 g, 3.35 mmol) were added to a stirred solution of methyl 4-phenylbicyclo[2.2.2]octane-1-carboxylate (0.78 g, 3.19 mmol) in CHCl₃ (20 mL). The resulting solution was stirred at ambient temperature for 90 min. The reaction mixture was poured into 5M sodium thiosulfate solution (100 mL) and extracted with CH₂Cl₂ (2 x 50 mL). The organic layer was washed with aqueous sodium thiosulfate (2 x 40 mL), separated and dried over Na₂SO₄. Volatiles were *in vacuo* and crude product was purified by silica gel flash silica chromatography (gradient of hexanes → 10% EtOAc/hexanes) to afford the desired product as a white solid (738 mg, 62 %).

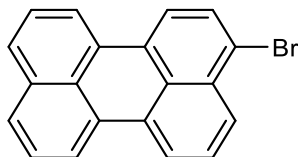
¹H NMR (400 MHz, CDCl₃): δ = 7.65 – 7.56 (m, 2H), 7.10 – 7.01 (m, 2H), 3.67 (s, 3H), 1.93 – 1.87 (m, 6H), 1.79 – 1.84 (m, 6H).

¹³C NMR (101 MHz, CDCl₃): δ = 173.45, 144.14, 132.37, 122.96, 56.27, 46.98, 34.25, 29.82, 26.80, 23.88.

HRMS (ESI+): *m/z* calcd for C₁₆H₁₉IO₂: 245.1542 (M-I+H)⁺, found: 245.1536.

m.p. = 99-102 °C.

f) 3-bromoperylene (8)



Anhydrous THF (120 mL) was added to a round-bottom flask containing perylene (1.0 g, 3.97 mmol). After complete dissolution, N-bromosuccinimide (0.7 g, 3.97 mmol) in 5 mL of anhydrous THF was added. The reaction mixture was stirred at room temperature under nitrogen atmosphere overnight where after 200 mL of water was added. The reaction mixture was extracted with CH₂Cl₂ (2 x 200 mL) and the organic phase washed with brine and dried over Na₂SO₄. Solvents were removed under reduced pressure to afford the title compound as a yellow solid (1.25 g, 95%), which was used without further purification. NMR Chemical shifts were in line with those published (31-33).

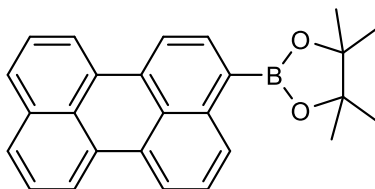
¹H NMR (400 MHz, CDCl₃): δ = 8.27-8.17 (m, 4H), 8.11 (d, J = 8.7 Hz, 1H), 8.02 (d, J = 8.4 Hz, 1H), 7.78 (d, J = 8.4 Hz, 1H), 7.73-7.67 (m, 2H), 7.62-7.57 (m, 1H), 7.53-7.47 (m, 2H).

¹³C NMR (101 MHz, CDCl₃): δ = 150.0, 134.6, 133.1, 131.6, 131.2, 130.7, 130.6, 130.4, 129.8, 128.4, 128.3, 127.9, 127.8, 122.3, 121.1, 120.9, 120.6, 120.5.

GC-MS (ESI+): m/z (M+H)⁺ = 330.

m.p. = 240-242 °C.

g) 3-(4,4,5,4-tetramethyl-1,3-dioxo-2-borolan-2-yl)perylene (9)



In a 250 mL Schlenk flask containing a mixture of 3-bromoperylene (1.0 g, 3 mmol), bis(pinacolato)-diboron (1.14 g, 4.5 mmol), Pd(dppf)₂Cl₂ (90 mg, 0.1 mmol, 5 mol%), potassium acetate (0.9 g, 9 mmol) was added anhydrous 1,4-dioxane (150 mL). The reaction mixture was purged with argon for 30 min and then stirred under an argon atmosphere at 80 °C for 17h. The flask was removed from heating bath and reaction mixture allowed to reach ambient temperature. Solvents were removed by rotary evaporation and the crude residue was purified by silica gel flash chromatography (isocratic toluene elution). The title pinacol ester was obtained as an orange powder (0.90 g, 80%). Spectroscopic properties were in line with those published (31, 34).

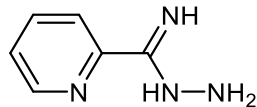
¹H NMR (400 MHz, CDCl₃): δ = 8.65 (d, J = 8.4 Hz, 1H), 8.26-8.17 (m, 4H), 8.06 (d, J = 7.5 Hz, 1H), 7.96 (t, J = 8.4 Hz, 2H), 7.56-7.46 (m, 3H), 1.43 (s, 12H).

¹³C NMR (101 MHz, CDCl₃): δ = 138.2, 136.1, 134.3, 133.8, 131.2, 131.0, 130.9, 130.8, 128.5, 128.3, 127.9, 127.8, 126.8, 126.7, 126.6, 120.9, 120.3, 120.2, 120.1, 119.3, 83.7, 24.9.

GC-MS (ESI+): m/z (M+H)⁺ = 378.

m.p. = 230-232 °C.

h) 2-pyridinyl hydrazonamide (11)



2-cyanopyridine (10.4 g, 0.1 mol) was placed in a round-bottom flask and dissolved 10 mL of absolute ethanol. Hydrazine hydrate (64-65%) (8.3 mL, 0.11 mol) was added portion wise at 0°C and reaction mixture was stirred overnight at room temperature. Afterwards, solvents were removed under reduced pressure, and the heterogeneous mixture was suspended in cold hexanes. Solids were filtered and collected on a glass frit, washing with cold hexanes to afford title compound (13 g, 95%) as a yellow fluffy solid with. ¹H NMR Chemical shifts were in line with those published (38, 39).

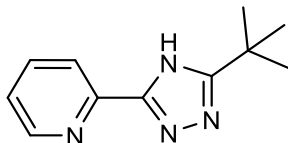
¹H-NMR (400 MHz, CDCl₃): δ = 8.51 (d, J = 6.00 Hz, 1H), 8.00 (d, J=6.00Hz, 1H), 7.71–7.65 (m, 1H), 7.28–7.23 (m, 1H), 5.27 (br-s, 2H), 4.49 (br-s, 2H).

¹³C-NMR (100 MHz, CDCl₃): δ = 150.64, 148.34, 147.70, 136.17, 123.54, 119.51.

GC-MS (ESI+): *m/z* (M+H)⁺ = 136.

m.p. = 95-97 °C.

i) 2-(5-(tert-butyl)-3H-1,2,4-triazol-3-yl)pyridine - (trzl-CMe₃) (12)



In a flame-dried, nitrogen-purged 30 mL Schlenk tube were placed (pyridine-2-yl)amidrazone (2.0 g, 15 mmol) and sodium carbonate (1.6 g, 15 mmol). The flask was evacuated and gently heated. After cooling, the flask was purged with nitrogen. Next, 15 mL of dry dimethylacetamide (DMAA) and 5 mL of dry THF were added, yielding a pale yellow suspension that was cooled to 0 °C. In a separate, dry 10 mL Schlenk flask, (1.8 g, 15 mmol) of the appropriate acid chloride was dissolved in 5 mL of DMAA. This solution was then added to precooled amidrazone mixture dropwise, which caused it to turn bright yellow. The mixture was slowly warmed to room temperature and stirred for additional 5 h, yielding a thick yellow mixture. The contents were filtered, the solid was washed with water and EtOH, and the resulting pale yellow solid was allowed to air dry. The solid was suspended in 20 mL of ethylene glycol and heated to 190 °C for 30 min, yielding a pale yellow solution. Upon cooling to room temperature, a white solid formed and was collected on a glass frit, washing with deionized water. The grey solid (1.83 g, 60%) was dried under vacuum and used without further purification. ¹H NMR Chemical shifts were in line with those published (40).

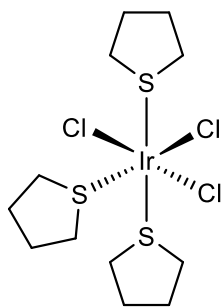
¹H-NMR (400 MHz, DMSO-d₆): δ = 8.71 (ddd, J = 4.8, 1.8, 1.0 Hz, 1H), 8.21 (dq, J = 7.9, 1.2 Hz, 1H), 7.83 (td, J = 7.8, 1.7 Hz, 1H), 7.35 (ddd, J = 7.6, 4.9, 1.2 Hz, 1H), 1.46 (s, 9H).

¹³C-NMR (101 MHz, CDCl₃): δ = 149.45, 137.23, 124.47, 121.74, 32.83, 29.51.

GC-MS (ESI+): *m/z* (M+H)⁺ = 202

m.p. = 192-194 °C.

j) $Ir(THT)_3Cl_3$ (14)



Compound **14** was synthesized according to literature procedure with a slight modification (41, 42).

To a room-temperature suspension of $IrCl_3 \cdot 3H_2O$ (2.00 g, 5.67 mmol) in 2-methoxyethanol (100 mL) was added tetrahydrothiophene (THT) (2.50 mL, 28.4 mmol). The solution was heated to reflux point for 12 h, subsequently the reaction mixture was allowed to cool and water (150 mL) was added to the room-temperature solution. Filtration provided crude product that was washed with precooled acetone to afford the title compound (2.74 g, 87%) as yellow microcrystals. 1H NMR Chemical shifts were in line with those previously published (41, 42).

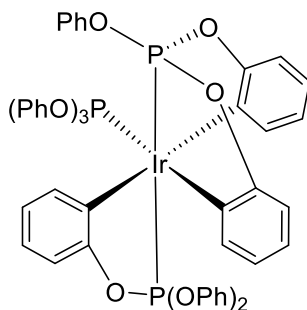
1H NMR (400 MHz, $CDCl_3$): δ = 3.64-3.58 (m, 4H), 3.23-3.17 (m, 2H), 2.91-2.80 (m, 6H), 2.30-2.01 (m, 12H).

^{13}C NMR (101 MHz, $CDCl_3$): δ = 36.92, 36.51, 30.49, 30.40.

Anal. calcd for $C_{12}H_{24}Cl_3IrS_3$: C, 25.60; H, 4.30; S, 17.08. Found: C, 25.6, H, 4.2, S, 17.0.

m.p. = 208-210 °C.

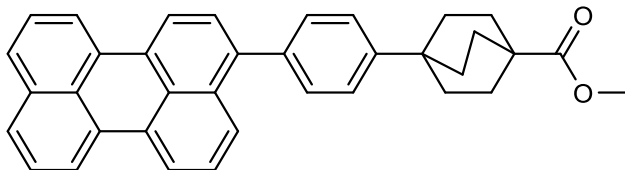
k) $Ir[P(OPh)_3](tpit)_2$ (15)



$Ir(THT)_3Cl_3$ (200 mg, 0.35 mmol), triphenyl phosphite (280 μ L, 1.06 mmol) and sodium acetate (292 mg, 3.56 mmol) were combined in decalin (16 mL). Reaction mixture was purged with argon for 30 min and then heated at 200 °C for 1 h in a microwave reactor. After cooling down solvents were removed under reduced pressure and crude residue was dry loaded on a silica packed column. Title compound was eluted with hexanes/EtOAc (1:3) affording (263 mg, 66%) as white fluffy solid.

1H NMR (800 MHz, $CDCl_3$): δ = 8.23 (t, J = 8.1 Hz, 1H), 7.83 (t, J = 8.1 Hz, 1H), 7.35 (t, J = 7.9 Hz, 2H), 7.28 (d, J = 8.0 Hz, 2H), 7.25 – 7.20 (m, 6H), 7.14 – 7.09 (m, 3H), 7.08 – 7.04 (m, 1H), 7.02 (d, J = 7.9 Hz, 3H), 7.00 – 6.91 (m, 13H), 6.91 – 6.89 (m, 2H), 6.88 (d, J = 7.2 Hz, 1H),

m) methyl 4-(4-(perylene-3-yl)phenyl)bicyclo[2.2.2]octane-1-carboxylate (17)



Methyl 4-(4-iodophenyl)bicyclo[2.2.2]octane-1-carboxylate (738 mg, 1.99 mmol), compound **9** (870 mg, 2.34 mmol) were placed in a 20 mL microwave vial. After addition of toluene (7 mL), 2M aqueous K_2CO_3 (5 mL), $Pd(PPh_3)_4$ (16.8 mg, 0.0146 mmol) and a few drops of Aliquat 336 the vial was capped and flushed with argon for 30 min. The reaction mixture was then stirred at 100 °C for 40 h. After cooling, the resulting mixture was washed with water and extracted with toluene. Purification by flash chromatography using toluene as an eluent afforded the product as a yellow solid (560 mg, 57%).

1H NMR (800 MHz, $CDCl_3$): δ = 8.19-8.24 (m, 4H), 7.79 (d, J = 8.30 Hz, 1H), 7.68 (d, J = 7.98 Hz, 2H), 7.48 (t, J = 7.73, 2H), 7.41-7.47 (m, 6H), 3.69 (s, 3H), 1.97 (s, 12 H)

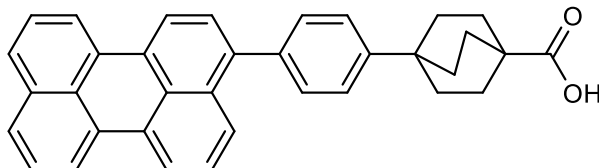
^{13}C NMR (201 MHz, $CDCl_3$): δ = 178.44, 148.33, 139.83, 138.06, 134.71, 132.98, 131.46, 131.38, 131.30, 130.47, 129.69, 129.08, 128.67, 127.76, 127.73, 127.69, 126.62, 126.42, 126.20, 125.50, 120.33, 120.29, 120.05, 119.96, 51.74, 39.13, 34.61, 31.80, 28.82.

HRMS (APCI+): m/z calcd for $C_{36}H_{30}O_2$: 495.2324 (M+H) $^+$; found 495.2335.

IR (V, cm^{-1}): 3026, 1604, 1495.

m.p. = 298-301 °C.

n) 4-(4-(perylene-3-yl)phenyl)bicyclo[2.2.2]octane-1-carboxylic acid (18)



In a 20-mL microwave vial, compound **10** (560 mg, 1.13 mmol) was suspended in THF (10 mL). A 2 M aqueous KOH solution (6.5 mL) was added and the vial was sealed with a Teflon liner cap and stirred vigorously at 80 °C for 48 h. The reaction mixture was then allowed to cool, transferred to a beaker containing 1N HCl (40 mL), and stirred for 15 min. The formed precipitate was collected on a glass frit and dried in vacuum overnight to yield the title compound (423 mg, 78%) as a canary yellow solid.

1H NMR (800 MHz, $DMSO-d_6$): δ = 12.06 (s, 1H), 8.41 (d, J = 7.6 Hz, 2H), 8.39 (dd, J = 7.6, 3.1 Hz, 2H), 7.81 (dd, J = 8.0, 3.3 Hz, 2H), 7.71 (d, J = 8.4 Hz, 1H), 7.56 (t, J = 7.7 Hz, 2H), 7.52 (t, J = 7.9 Hz, 1H), 7.50 (d, J = 8.2 Hz, 2H), 7.44 (dd, J = 10.6, 7.8 Hz, 3H), 1.86 (ddt, J = 15.6, 11.7, 6.0 Hz, 12H).

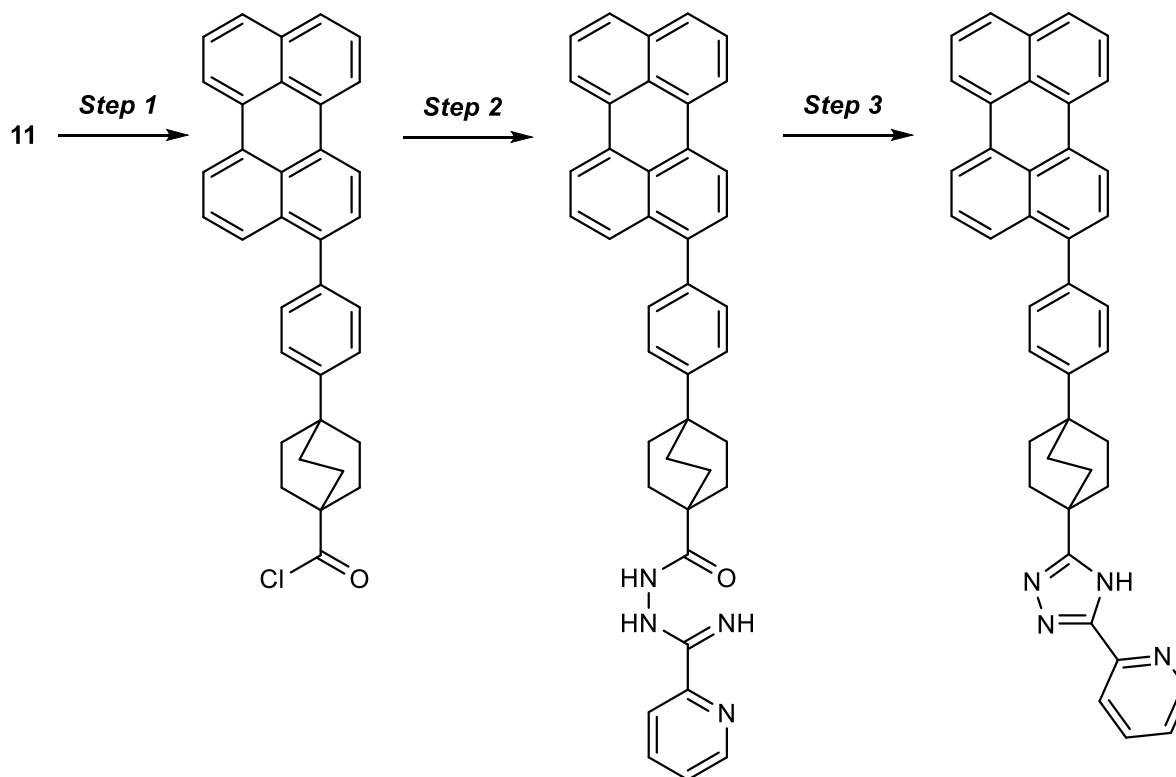
^{13}C NMR (201 MHz, $DMSO-d_6$): δ = 184.03, 153.77, 144.49, 142.33, 139.52, 137.45, 136.05, 135.83, 135.66, 135.03, 134.58, 133.56, 133.21, 133.14, 133.07, 133.04, 132.27, 132.21, 130.89, 126.14, 125.88, 125.74, 43.27, 39.50, 36.54, 33.67.

HRMS (ESI+): m/z calcd for $C_{35}H_{28}O_2$: 481.2162 (M+H) $^+$; found 481.2159.

IR (V, cm^{-1}): 2957, 1449, 1429.

m.p. (dec.) = 336-338 °C.

o) 2-(5-(4-(4-(perylene-3-yl)phenyl)bicyclo[2.2.2]octan-1-yl)-4H-1,2,4-triazol-3-yl)pyridine (**19**)



Step 1:

Compound **11** (260 mg, 0.541 mmol) was suspended in oxalyl chloride (10 mL) containing catalytic amount of anhydrous DMF. Gas evolution occurred and stirring continued for 2 h under a CaCl₂ drying tube. Excess of oxalyl chloride was removed under reduced pressure and the corresponding acid chloride was used immediately in the next step without any further purification or characterization.

Step 2:

In an oven-dried 20 mL Schlenk vial were placed (pyridine-2-yl)-amidrazone (88.3 mg, 0.65 mmol) and sodium carbonate (57.34 mg, 0.541 mmol). The flask was evacuated and gently heated, after cooling it was backfilled with nitrogen. Next, anhydrous DMAA (5 mL) and anhydrous THF (3 mL) were added, yielding a pale-yellow suspension that was cooled to 0 °C. In a separate anhydrous 10 mL Schlenk flask (270 mg, 0.541 mmol) of acid chloride was suspended in 5 mL of DMMA. This suspension was then added to a precooled amidrazone mixture dropwise. The mixture was slowly warmed to room temperature and stirred for additional 5 h, yielding a thick hazel brown mixture. Contents were filtered, the solid was washed with water and EtOH, and the resulting yellow solid was air dried.

Step 3:

Obtained material was suspended in ethylene glycol (8 mL) and heated to 200 °C for 2 h. After cooling the reaction mixture was filtered and the formed yellow solid was collected on a glass frit and washed with deionized water and ethanol. Crude material was purified by flash

chromatography using silica packed column eluting with CH₂Cl₂/MeOH (95:5) to afford title compound as a yellow solid (148 mg, 46%).

¹H NMR (800 MHz, DMSO-d₆): δ = 14.33 (s, 0.58H), 13.85 (s, 0.42H), 8.67 (d, *J* = 43.1 Hz, 1H), 8.48 – 8.36 (m, 7H), 8.06 (dd, *J* = 18.7, 7.7 Hz, 1H), 7.99 (t, *J* = 7.9 Hz, 1H), 7.89 (s, 1H), 7.82 (dd, *J* = 8.1, 3.1 Hz, 2H), 7.75 (d, *J* = 8.4 Hz, 1H), 7.65 – 7.46 (m, 9H), 2.08 (m, 6H), 2.02 (m, 6H).

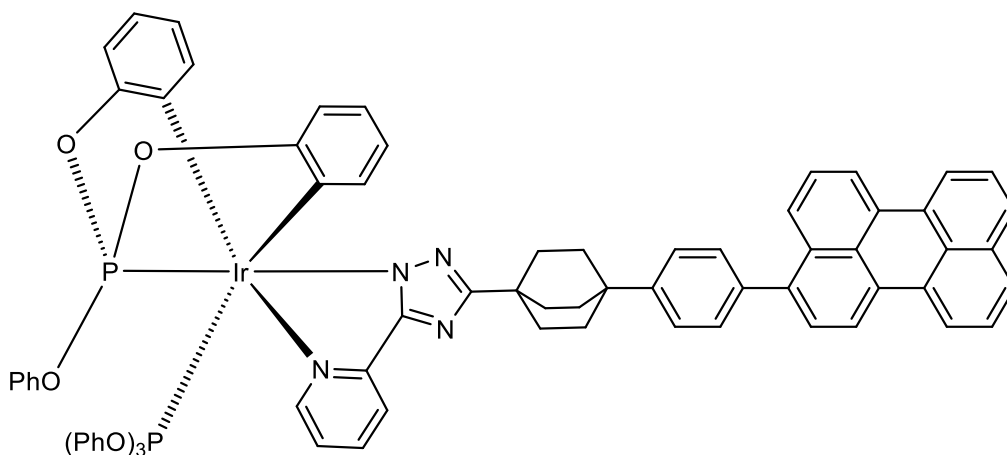
¹³C NMR (201 MHz, DMSO-d₆): δ = 177.76, 173.23, 163.96, 150.68, 148.87, 148.66, 143.65, 139.80, 138.20, 137.83, 137.71, 134.83, 132.83, 131.37, 131.16, 130.99, 130.37, 130.34, 129.88, 129.81, 128.91, 128.40, 128.32, 128.28, 127.44, 127.42, 127.39, 126.60, 126.09, 126.05, 123.30, 121.32, 121.06, 120.92, 79.59, 79.42, 79.26, 63.35, 51.88, 34.76, 32.83, 31.90, 31.75, 31.60, 30.10, 29.01, 28.96.

HRMS (ESI+): *m/z* calcd for C₄₁H₃₂N₄: 581.2700 (M+H)⁺; found 581.2705.

IR (V, cm⁻¹): 3425, 2957, 1449, 1429.

m.p. (dec.) = 366-369 °C.

p) Ir[P(OPh)₃](tpit)(bco[2.2.2]-1,4-Ph-3-Perylene) (**20**)



Complex **17** (101 mg, 0.09 mmol) was placed in a microwave vial containing compound **14** (52.3 mg, 0.09 mmol), sodium acetate (73.8 mg, 0.9 mmol) where after a mixture of decalin/ODCB (2:1) (20 mL) was added. Microwave vial was sealed with a Teflon liner cap and reaction mixture purged with argon for 30 min and then heated at 250 °C for 6h in a microwave reactor. After cooling down solvents were removed under reduced pressure and crude residue was dry loaded on a silica column. Title compound was eluted with CH₂Cl₂/MeOH (97:3) affording (46.5 mg, 37 %) as yellow powder.

¹H NMR (800 MHz, CDCl₃): δ = 9.30 – 9.05 (m, 1H), 8.37 – 8.13 (m, 5H), 8.00 (d, *J* = 7.8 Hz, 1H), 7.86 (d, *J* = 8.3 Hz, 1H), 7.68 (dd, *J* = 8.1, 2.4 Hz, 2H), 7.57 (dd, *J* = 7.9, 5.2 Hz, 4H), 7.54 – 7.40 (m, 10H), 7.35 (t, *J* = 7.4 Hz, 1H), 7.05 (t, *J* = 7.9 Hz, 7H), 7.00 (dd, *J* = 8.2, 6.5 Hz, 3H), 6.94 (dd, *J* = 7.0, 1.7 Hz, 2H), 6.84 (dd, *J* = 7.2, 1.8 Hz, 1H), 6.75 (dd, *J* = 7.9, 3.6 Hz, 1H), 6.69 (t, *J* = 7.2 Hz, 1H), 6.55 (ddd, *J* = 7.1, 5.6, 1.3 Hz, 1H), 6.44 (d, *J* = 8.0 Hz, 7H), 5.77 (t, *J* = 8.4 Hz, 1H), 2.37 (q, *J* = 6.2 Hz, 6H), 2.14 (t, *J* = 7.7 Hz, 6H).

¹³C NMR (201 MHz, CDCl₃): δ = 172.96, 162.69, 159.65, 159.58, 158.48, 152.81, 151.09, 151.03, 150.14, 149.70, 140.13, 137.87, 137.71, 137.46, 134.72, 133.45, 133.05, 131.54, 131.39, 131.33, 130.35, 130.08, 129.61, 129.42, 129.09, 128.70, 127.77, 127.70, 127.62, 126.63, 126.60,

126.40, 125.85, 125.70, 125.34, 124.63, 124.48, 123.45, 123.41, 123.17, 122.79, 120.98, 120.83, 120.43, 120.42, 120.33, 120.25, 120.01, 114.78, 110.96, 110.88, 110.76, 35.23, 33.60, 32.82, 31.94, 29.70, 26.92.

^{31}P NMR (162 MHz, CDCl_3): δ = 124.28 (d, J = 23.9 Hz, 1P), 75.09 (d, J = 24.0 Hz).

HRMS (ESI+): m/z calcd for $\text{C}_{77}\text{H}_{59}\text{IrN}_4\text{O}_6\text{P}_2$: 1391.3617 ($\text{M}+\text{H}$) $^+$; found 1391.3615.

IR (V , cm^{-1}): 3047, 2953, 2918, 2862, 1614, 1590, 1488, 1452, 1431.

m.p. = 283-286 °C.

Section S2. Details of the experimental determination of the rate of energy transfer

The rate of energy transfer (or rate of emission), k , can be calculated from the quantum yield of energy transfer, Φ , (or quantum yield of emission) and the corresponding excited state lifetime, τ

$$k = \frac{\Phi}{\tau} \quad (1)$$

Figures 3A-C show the excited state decay from D, A, and DBA, and the fitted lifetimes together with the associated emission quantum yields are summarized in Table S1. DBA emission is due to two processes: firstly from direct excitation of the acceptor part, secondly from excitation of the donor part followed by energy transfer to the acceptor from where emission occurs (it should be noted that no emission occurs from the donor moiety, see Fig. 3E). The quantum yield of emission from DBA, can thus be divided into fractional contributions (f_1 and f_2) arising from direct excitation, and FRET followed by A emission. The quantum yield of Förster type resonance energy transfer is therefore

$$\Phi_{\text{FRET}} = \frac{\Phi_{\text{DBA}} \cdot f_2}{\Phi_{\text{A}}} \quad (2)$$

Furthermore, it can be assumed that the rate of energy transfer is slower compared to A emission, the second lifetime of DBA ($\tau_{\text{DBA},2}$) therefore reflect the lifetime of energy transfer and the rate of energy transfer is

$$k_{\text{FRET}} = \frac{\Phi_{\text{FRET}}}{\tau_{\text{FRET}}} = \frac{\Phi_{\text{DBA}} \cdot f_2}{\Phi_{\text{A}} \cdot \tau_{\text{DBA},2}} \quad (3)$$

Resulting in values for the rate of emission from the donor and acceptor moieties of $1.93 \cdot 10^4 \text{ s}^{-1}$ and $2.7 \cdot 10^8 \text{ s}^{-1}$, respectively, and a rate of energy transfer of $5.33 \cdot 10^5 \text{ s}^{-1}$. It should be noted that the quantum yield of emission from the dyad is lower as compared to the quantum yield of donor emission (when excited at the same wavelength). However, when exciting at longer wavelength, where only the acceptor absorbs, the quantum yield is roughly the same between the dyad and the acceptor. Thus, a new non-radiative decay pathway has opened up in the dyad, accessible from the excited triplet state of the donor, but not from the excited singlet state of the acceptor.

Table S1. Excited-state lifetimes (fractional contributions in parentheses) and associated emission quantum yields for D, A, and DBA in toluene solutions. Excitation wavelengths were 320 nm, 405 nm and 320 nm for D, A and DBA, respectively. It should be noted that the lifetime and the quantum yield of the donor are somewhat lower as compared earlier reports using dichloromethane as a solvent (24).

Molecule (λ_{ex})	τ_1 (f_1)	τ_2 (f_2)	χ^2_{R}	Φ
D (320 nm)	$41.5 \pm 31 \cdot 10^{-3} \text{ } \mu\text{s}$		1.37	0.62
A (405 nm)	$3.09 \pm 3 \cdot 10^{-3} \text{ ns}$		1.09	0.85
DBA (320 nm)	$3.74 \pm 11 \cdot 10^{-3} \text{ ns}$ (0.497)	$289.54 \pm 0.99 \text{ ns}$ (0.503)	1.26	0.26
DBA (405 nm)	$3.03 \pm 2 \cdot 10^{-3} \text{ ns}$		1.02	0.82

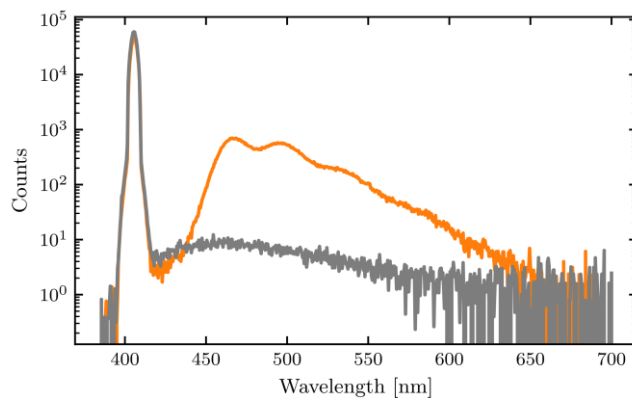


Fig. S1. Emission quantum yield of A, measured using an integrated sphere. Sample was dissolved in toluene.

Regarding the biphasic decay of Fig. 3C, we argue that the short component is due to a direct excitation of the perylene moiety. To confirm that is indeed a direct excitation, we compare the ratio between the fractional contributions of the dyad decay ($f_2/f_1 = 1.01$) with molar absorptivities of both the donor, the acceptor and the quantum yield

$$\frac{\varepsilon_D}{\varepsilon_A} \cdot \Phi_{\text{FRET}} = 0.88 \quad (4)$$

Where, ε_D and ε_A are the molar absorptivities of the donor and the acceptor at 320 nm, respectively. Φ_{FRET} is given by equation S2.

The new non-emissive decay process was confirmed to be triplet triplet energy transfer (TET) from D to A using nanosecond transient absorption measurements. An excited state absorption peak at 375 nm was observed after laser excitation at 320 nm of a toluene solution of D (fig. S2A). The decay lifetime of the excited state absorption at 375 nm was 29.6 μs , which is close to the phosphorescence lifetime of D (fig. S2B). We can then assign the excited state absorption at 375 nm to the $T_1 - T_n$ transition of D.

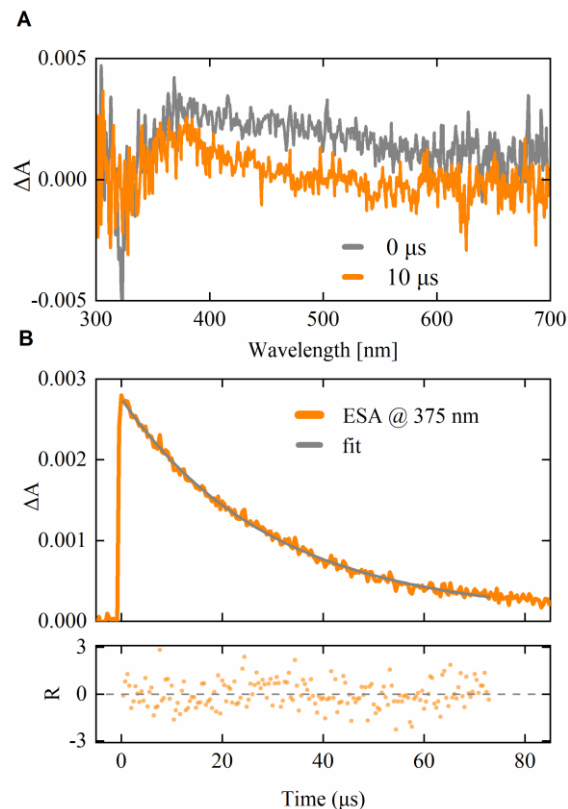


Fig. S2. Transient absorption spectroscopy and decay of D in toluene when excited at 320 nm. (A) Transient absorption spectroscopy of D in toluene when excited at 320 nm; (B) Transient absorption decay of D at 375 nm.

Figure S3 show the transient absorption spectrum of DBA in toluene solution. After laser excitation at 320 nm, the $T_1 - T_n$ transition of D now decreases in a few hundreds of nanoseconds, while a strong more long-lived transient absorption peak is formed at 485 nm. The excited state absorption peak at 485 nm is attributed to the $T_1 - T_n$ transition of acceptor perylene.⁽⁴³⁾ The excited state absorption lasts for more than 50 microseconds, which is in accordance with the slow non-radiative decay of the perylene triplet state.

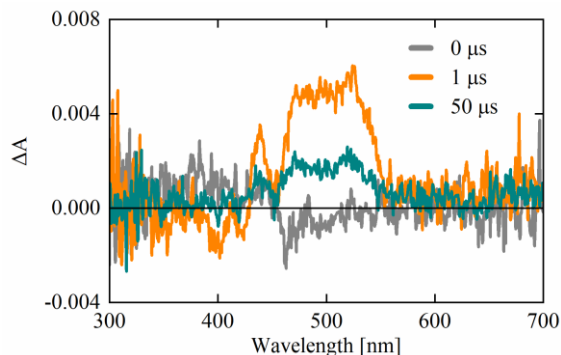


Fig. S3. Transient absorption spectroscopy of DBA in toluene solution when excited at 320 nm.

Figure S4 shows the decay kinetics of the transient absorption peaks at 375 and 485 nm of DBA in toluene. When exciting DBA at 320 nm, the lifetimes of transient absorption at 375 nm ($T_1 - T_n$

transition of D) and 485 nm (T_1 - T_n transition of A) are 288 ns and 51.6 μ s, respectively. The rate constant of triplet-triplet energy transfer (k_{TET}) in DBA was calculated as

$$k_{\text{TET}} = \frac{1}{\tau_{\text{DBA}_2}} - \frac{1}{\tau_{\text{D}}} - k_{\text{FRET}} = 2.89 \times 10^6 \text{ s}^{-1} \quad (5)$$

where τ_{D} and τ_{DBA_2} are decay lifetimes of mere D and D in the DBA dyad.

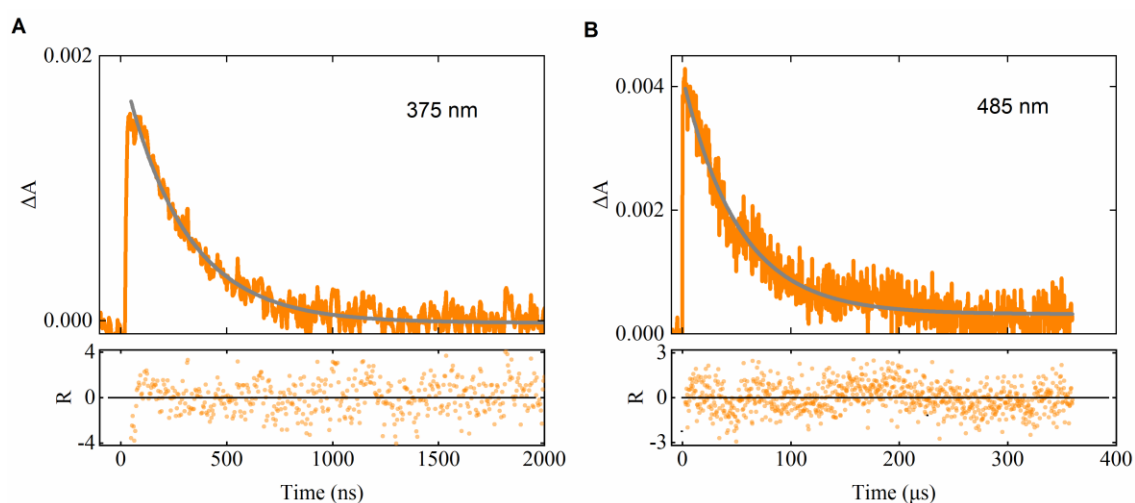


Fig. S4. Transient absorption decays of DBA when excited at 320 nm. Transient absorption decays of DBA excited at 320 nm and measured at (A) 375 nm and (B) 485 nm.

Section S3. Details of the simulation of the rate of energy transfer

The theoretical foundation of resonance energy transfer was developed by Theodore Förster in 1948 (12). The energy is transferred from a donor D to an acceptor A molecule. The transition dipole moment (μ) of the donor and acceptor is modelled as two oscillating dipoles. The interaction between the dipoles is approximated by electrostatic forces, resulting in a six power of the donor-acceptor distance, r , on the rate of energy transfer, k_T

$$k_T(r) = k_D \frac{0.211^6 \kappa^2}{n^4 r^6} \int_0^\infty F_D(\lambda) \epsilon_A(\lambda) \lambda^4 d\lambda \quad (6)$$

where k_D is the radiative rate constant of the donor in the absence of acceptor, n is the refractive index of the medium, r is the donor-acceptor distance, and κ^2 describes the relative orientation in space of the transition dipoles of the donor and acceptor. The integral describes the energy matching of the oscillating dipoles, in which F_D is the area normalized emission of the donor, and ϵ_A is the extinction coefficient of the acceptor.

The simulated rate of energy transfer was calculated using Equation S6. The refractive index was set to 1.496, and the overlap integral was calculated using the data in Fig. 2 and Fig. 3E ($J=2.16 \cdot 10^{14} \text{ M}^{-1} \text{ cm}^{-1} \text{ nm}^4$). The bridging unit between the donor and acceptor moieties is rigid preventing bending. However, there is rotational degrees of freedom in the bridging unit. The donor-acceptor distance, r , as well as the orientation factor, κ^2 , is therefore a function of bridge rotation. To calculate r and κ^2 , the structure of DBA in Fig. 1A was used, which is based on the crystal structure of D with the addition of the crystal structure of the ligand, **19**, and the dihedral $\text{C}_{\text{phenyl}}\text{-C}_{\text{phenyl}}\text{-C}_{\text{bicyclooctane}}\text{-C}_{\text{bicyclooctane}}$ angle in the bridge was changed to capture the effect of the free rotation in solution. The transition dipole moment of the first excited singlet state of perylene is located in the long axis direction of the molecule (44), and since the chromophore is symmetric, the centre of gravity was set to the centre point of the chromophore in the analysis. The transition responsible for phosphorescence in the donor is a metal to ligand (pyridyl) charge transfer. The centre of gravity was set to be between Ir and the pyridyl N, with a direction of the transition dipole moment in-between those two atoms. The κ^2 value was calculated using (45)

$$\kappa^2 = (\cos \theta_T - 3 \cos \theta_D \cos \theta_A)^2 \quad (7)$$

Where θ_T , θ_D , and θ_A is the angle between the vectors $\vec{\mu}_D$ and $\vec{\mu}_A$, $\vec{\mu}_D$ and \vec{r} , and $\vec{\mu}_A$ and \vec{r} , respectively (where $\vec{\mu}$ is the transition dipole moment). The simulated rate of energy transfer as a function of dihedral angle is shown in fig. S5 Furthermore, the rotation around the single bonds in the bridge can be assumed to occur much faster as compared to the timescale of energy

transfer, meriting the use of an average value of the rate of energy transfer as mentioned in the main text.

The unidirectionality of the energy transfer is best quantified by the ratio of the overlap integrals between the forward ($D^*+A \rightarrow D+A^*$) and backward ($D+A^* \rightarrow D^*+A$) energy transfer reactions. The overlap integral is for the forward reaction $2.16 \cdot 10^{14} \text{ M}^{-1} \text{ cm}^{-1} \text{ nm}^4$, and for the backward reaction $6.49 \cdot 10^{12} \text{ M}^{-1} \text{ cm}^{-1} \text{ nm}^4$, giving a ratio of 33 for the energy requirement for energy transfer to occur.

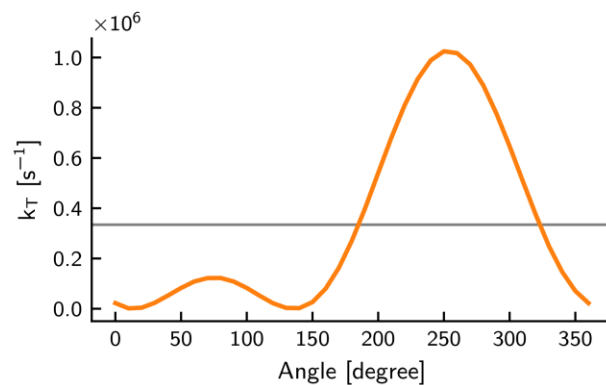


Fig. S5. The simulated rate of energy transfer as a function of dihedral angle (orange line). The average simulated value is shown as a grey line.

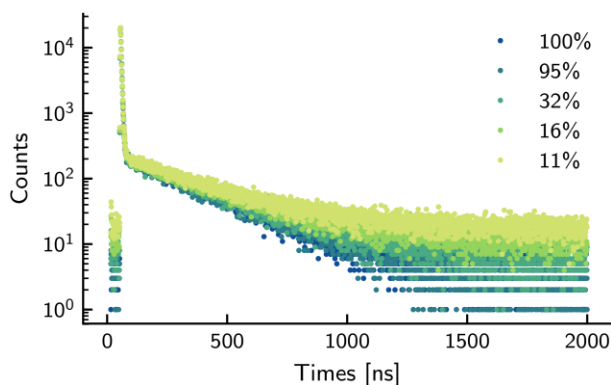


Fig. S6. Lifetime of DBA with different excitation intensity. The scale of the intensity is normalized to the maximum, then the intensity is reduced using a neutral density filter. The intensity is measured by recording the signal rate on the MCS detector. All lifetimes from the long tail part are, within margin of error, 300 ns (baseline was corrected for each decay).

Section S4. X-ray diffraction of 19 and DBA

The ligand (19)

X-ray diffraction data were collected at beamline BioMAX at the MAX IV Laboratory in Lund, Sweden. The crystal was rotated a full 360 degree turn on a micro-diffractometer MD3, equipped with an EIGER 16M detector (4150*4371 pixel) at a detector-crystal distance of 158.5 mm. The chosen wavelength was 0.82656 Å. In total 3600 images were collected with a 10 ms exposure time each, giving 36 s total data collection time, at 20% beam transmission. The integration of the collected images were done with XDS (46), a standard macromolecular software suite for integration. The structure were solved with SHELXT (47) and slightly edited with respect to atom type assignments. The refinements were done with SHELXL (47). All atoms were refined with anisotropic displacement parameters and the hydrogen atoms were geometrically placed with respect to the other atoms. The hydrogens were restrained at a standard distance available in SHELXL. The unusually high R-values, $R1 = 0.142$ is most probably related to partial saturation of the detector. This is detectable in quite large spread of intensities between several reflections that should have been given equal intensities. However the residual densities are very small, in the range $[-0.34 - 0.41] \text{ e}/\text{Å}^3$. Crystal data have been deposited with the Cambridge Crystallographic Data Centre with the code CCDC-1886199.

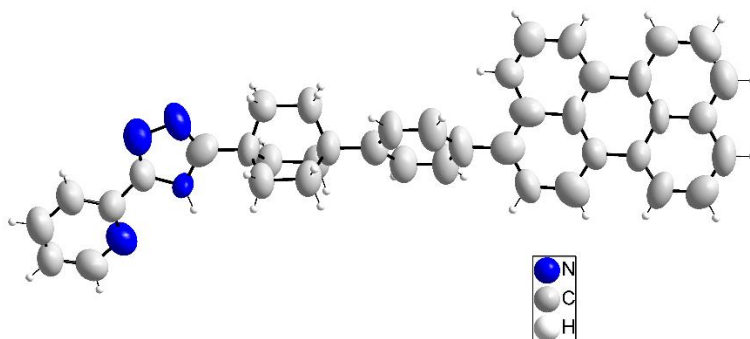


Fig. S7. Structure of the ligand (19), as solved by x-ray diffraction.

DBA (20)

X-ray diffraction data were collected with a Bruker Advance D8 equipped with a Photon 100 detector and an Incotec 1MyS Cu microsource. The crystal was subjected both to phi scans as well as omega scans in order to cover Ewald sphere up to 133 degrees two-theta. The wavelength was 1.54184 Å and the total data collection time was 24 h. The integration of the collected images were done with the CrysAlis software from Rigaku/Oxford Diffraction clearly indicated a modulated structure with satellites visible. However, we have been unable to use the satellite reflection due to low intensity, thus we present an average structure from the main reflections extracted from the full dataset. The structure was solved from main reflections with SHELXT and slightly edited with respect to atom type assignments. The refinements were done with SHELXL. All atoms were refined with anisotropic displacement parameters and the hydrogen atoms were geometrically placed with respect to the other atoms and constrained to a standard bonding distance available in SHELXL. The heavy anisotropy of the displacement ellipsoids indicates that the average 3d structure only is an approximate description. The high R-values, $R1 = 0.118$ is related to the fact that we have refined the structure model as a traditional 3d-model while it should be done in at least a (3+1)d space group. The residual densities $[-2.03 - 1.60]$ $e/\text{Å}^3$ also indicates the need for a better structure description. Crystal data have been deposited with the Cambridge Crystallographic Data Centre with the code CCDC 1886229. Diffraction data for the Ir-complex has been measured at a synchrotron installation with clearly much better counting statistics than from our in house X-ray source, however the data from the very modern detector (EIGER 16M) seems not (yet) to be readable by the CrysAlis software.

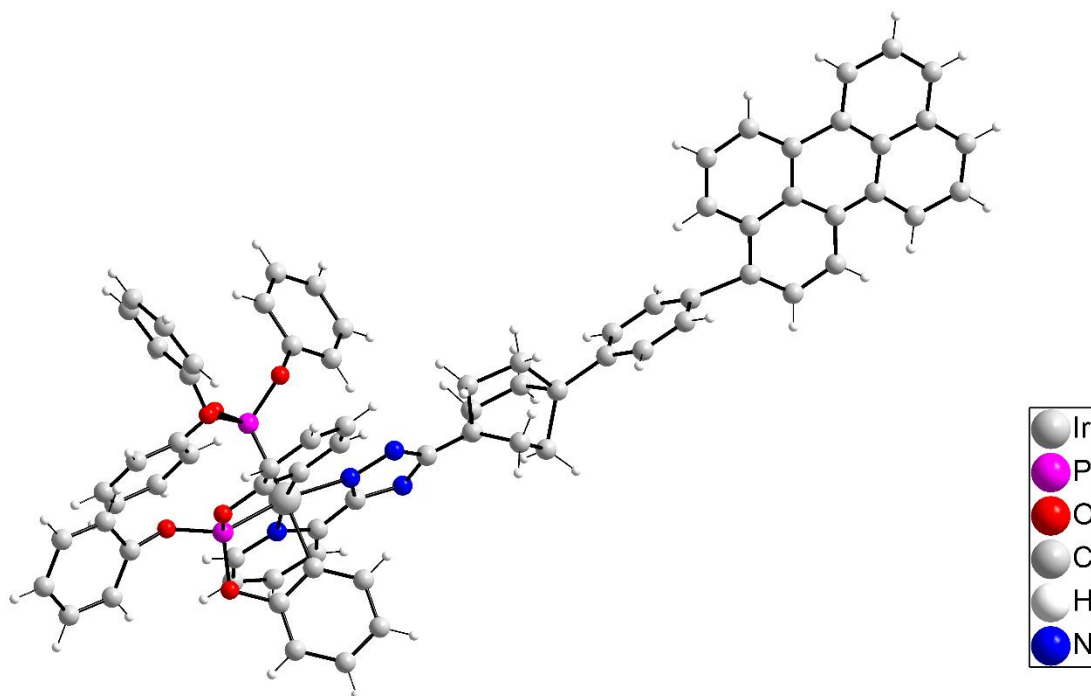


Fig. S8. Structure of DBA (20), as solved by x-ray diffraction.

NMR spectra

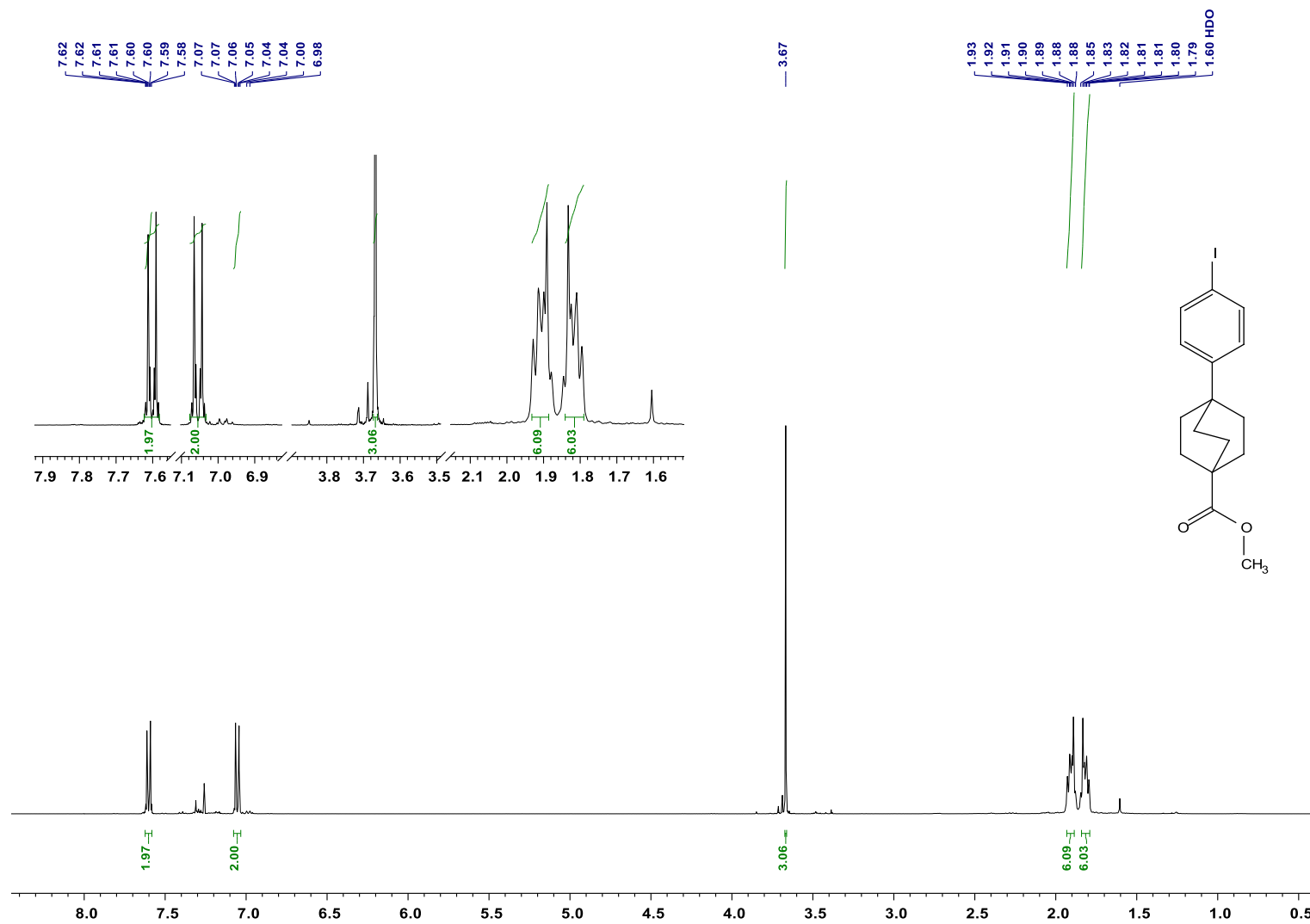


Fig. S9. ¹H NMR (400 MHz, CDCl₃), 6.

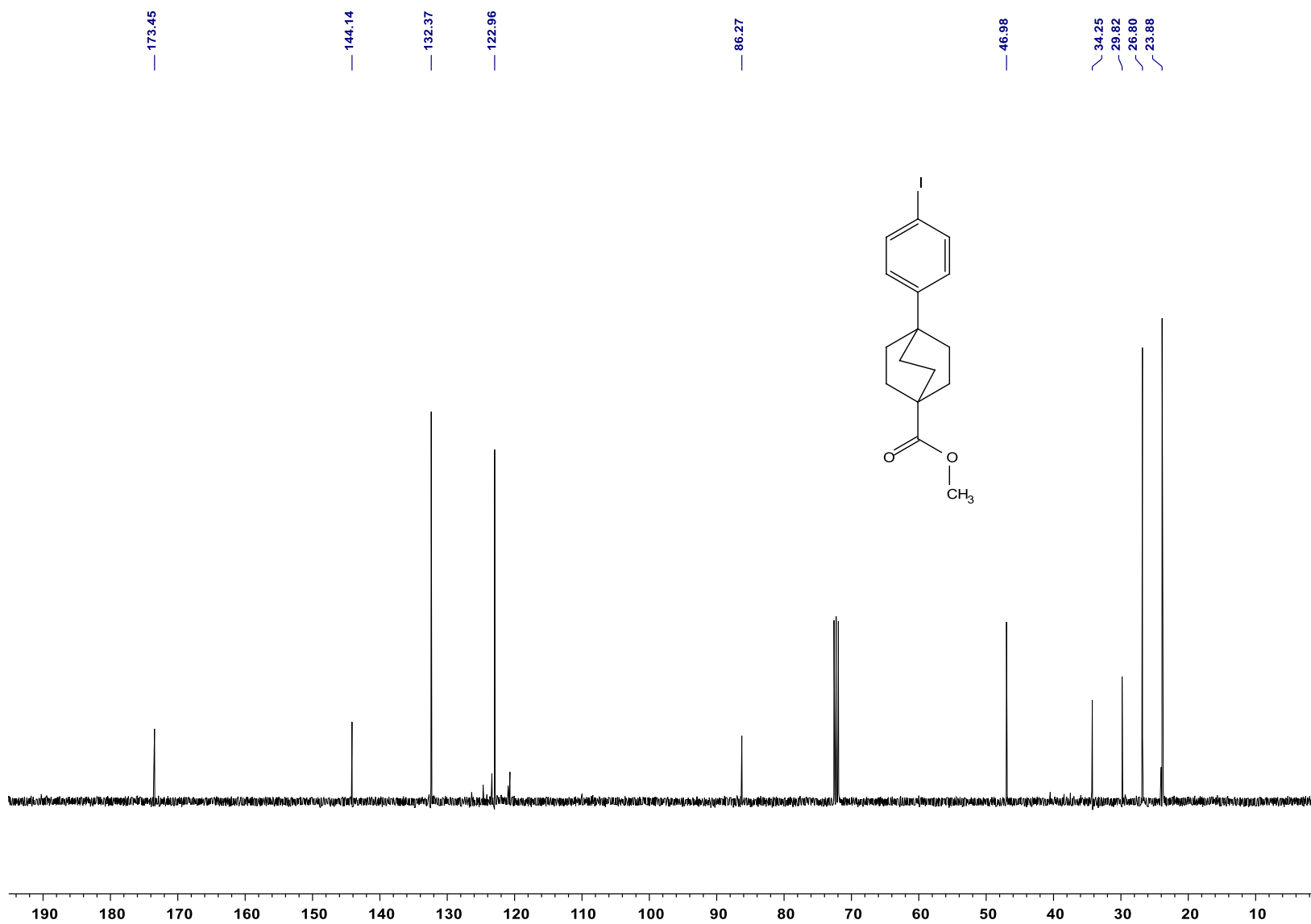


Fig. S10. ^{13}C NMR (101 MHz, CDCl_3), 6.

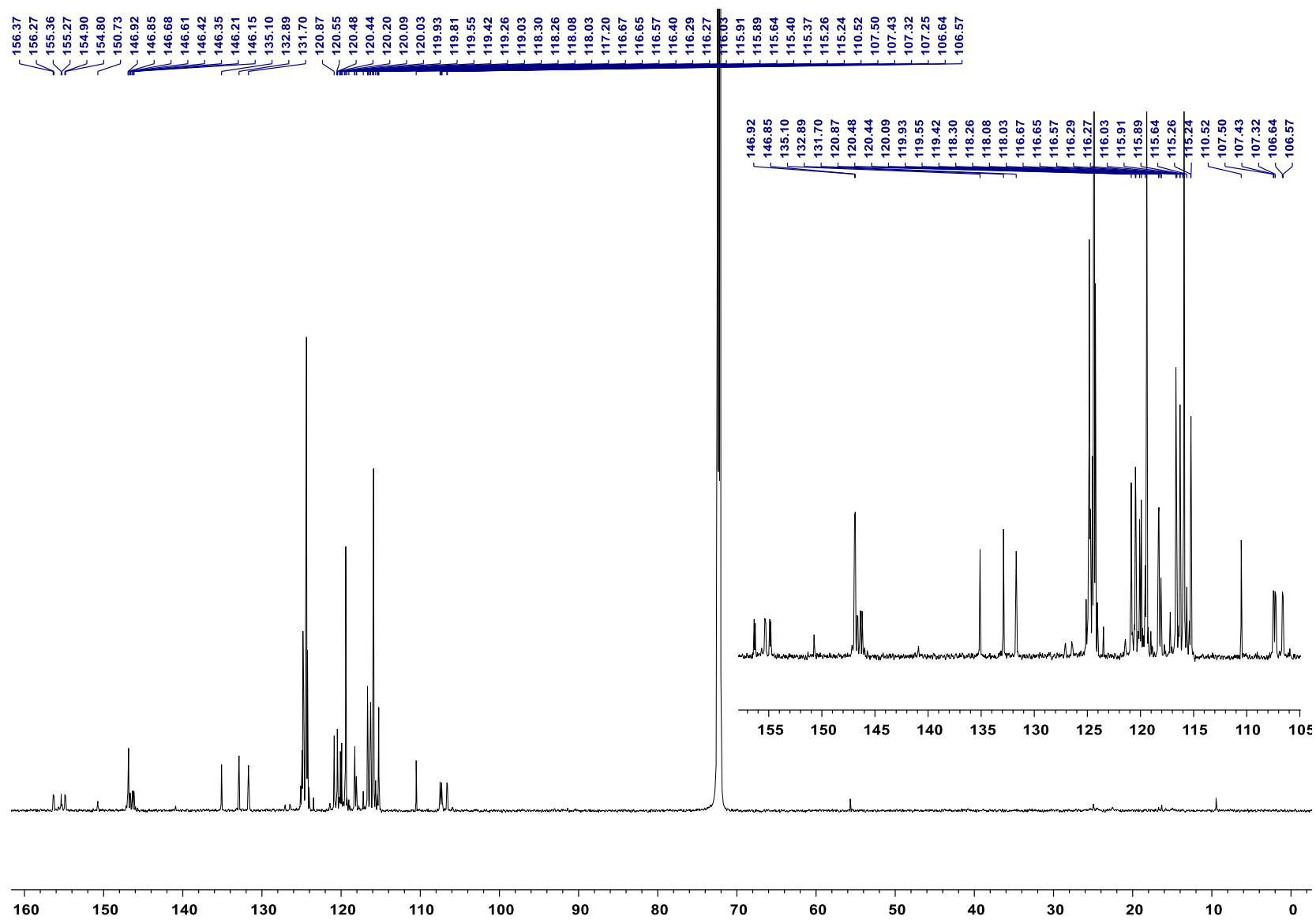


Fig. S12. ^{13}C NMR (201 MHz, CDCl_3), 15.

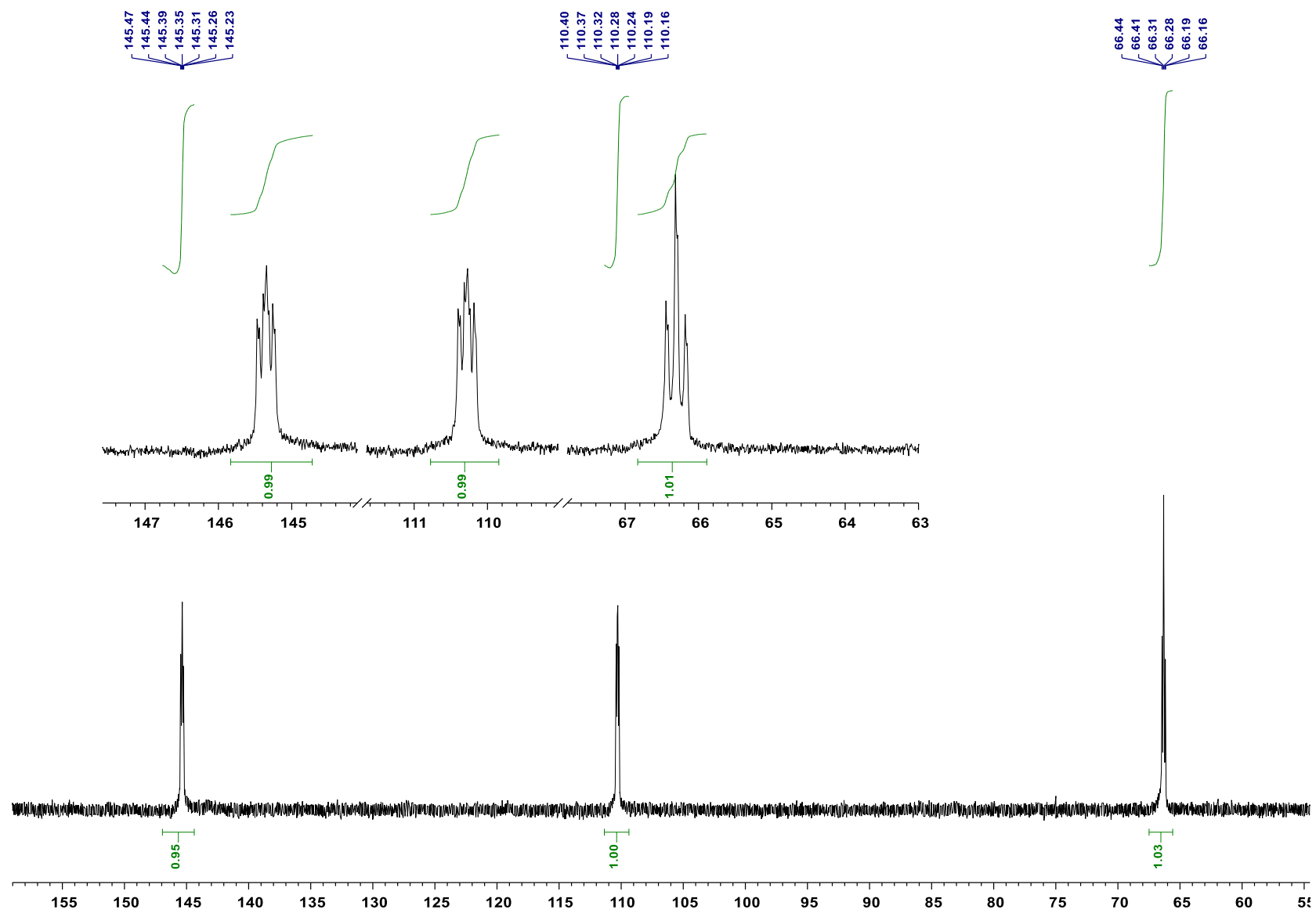


Fig. S13. ^{31}P NMR (162 MHz, CDCl_3), 15.

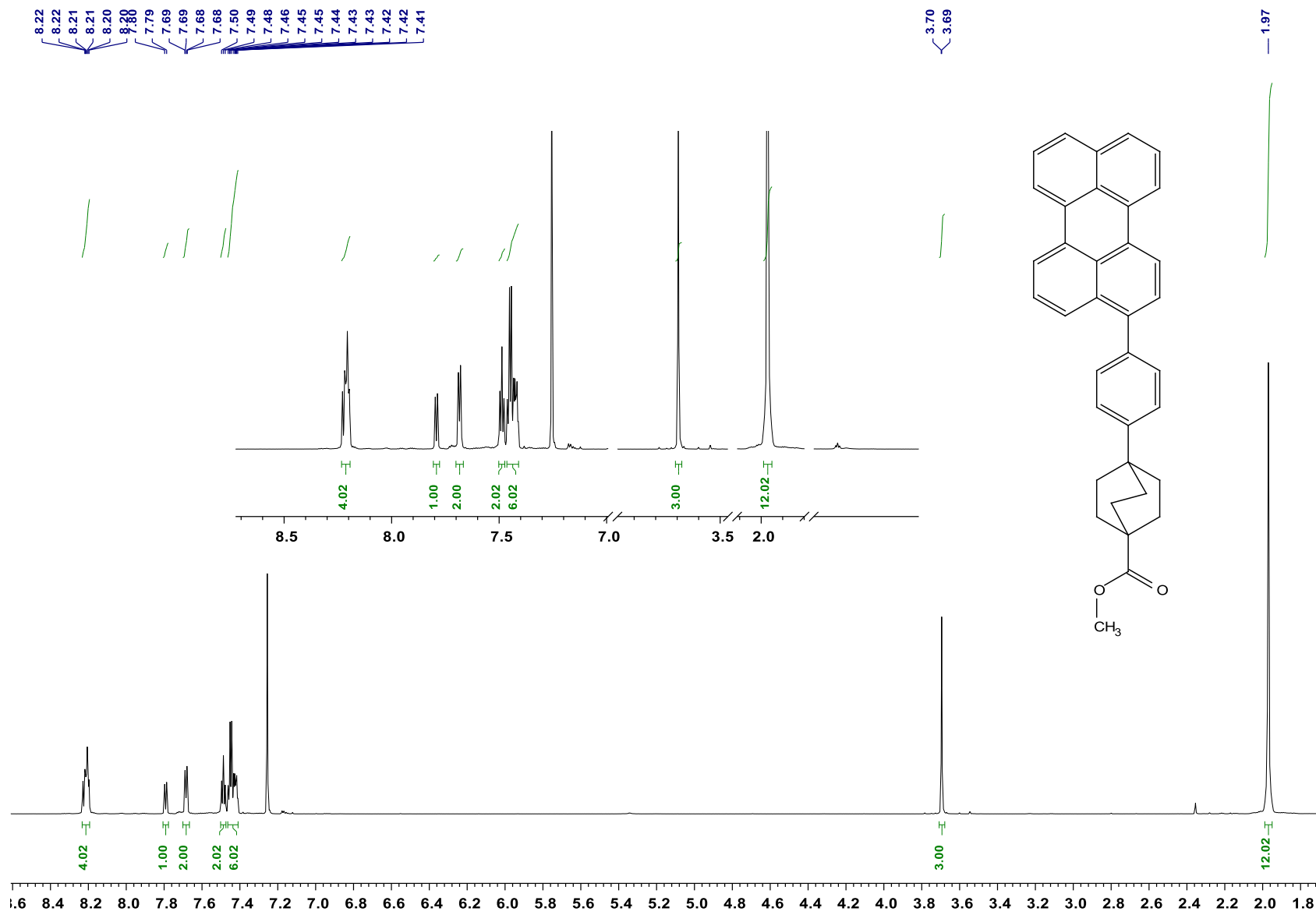


Fig. S14. ¹H NMR (800 MHz, CDCl₃), 17.

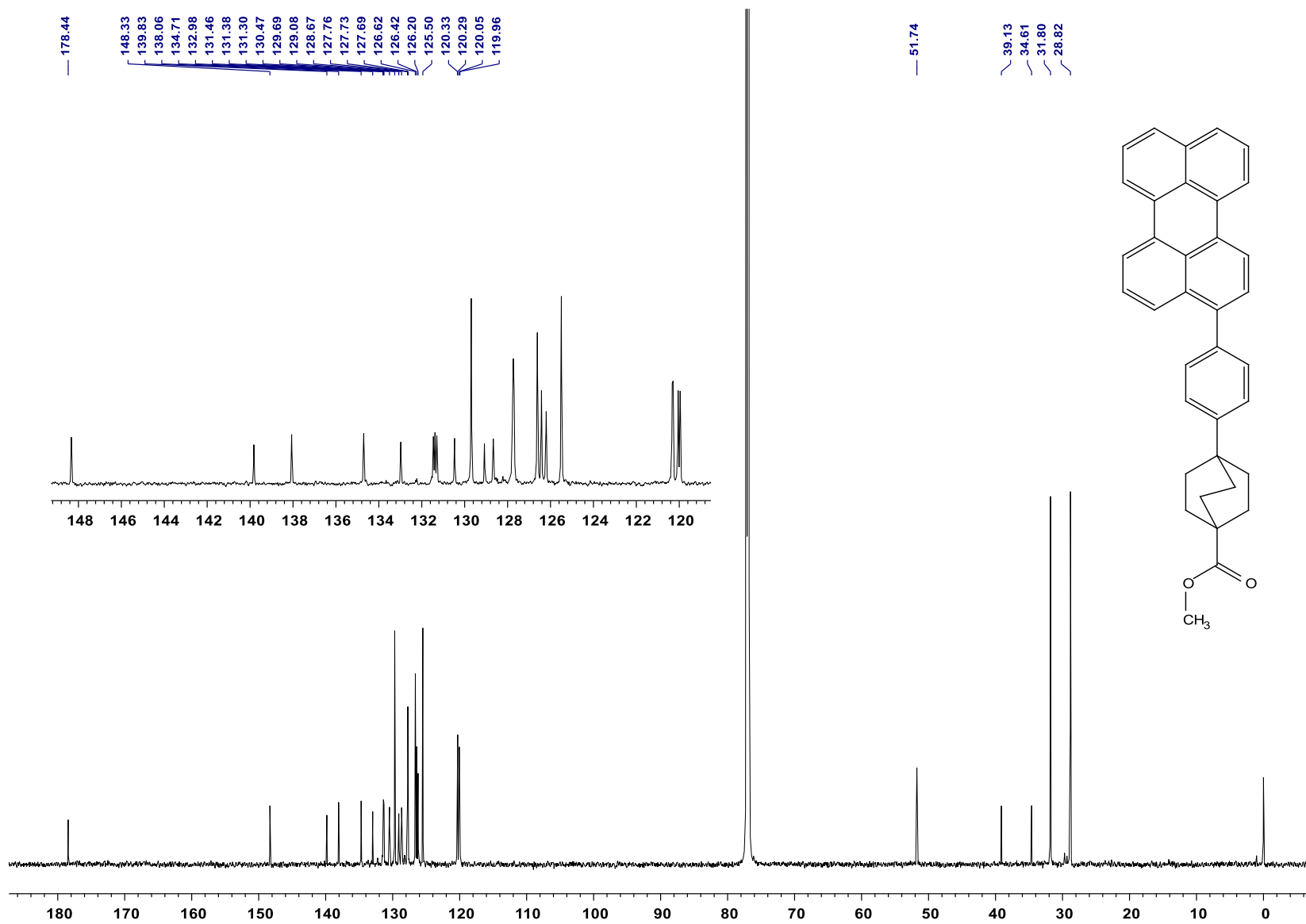


Fig. S15. ^{13}C NMR (201 MHz, CDCl_3), 17

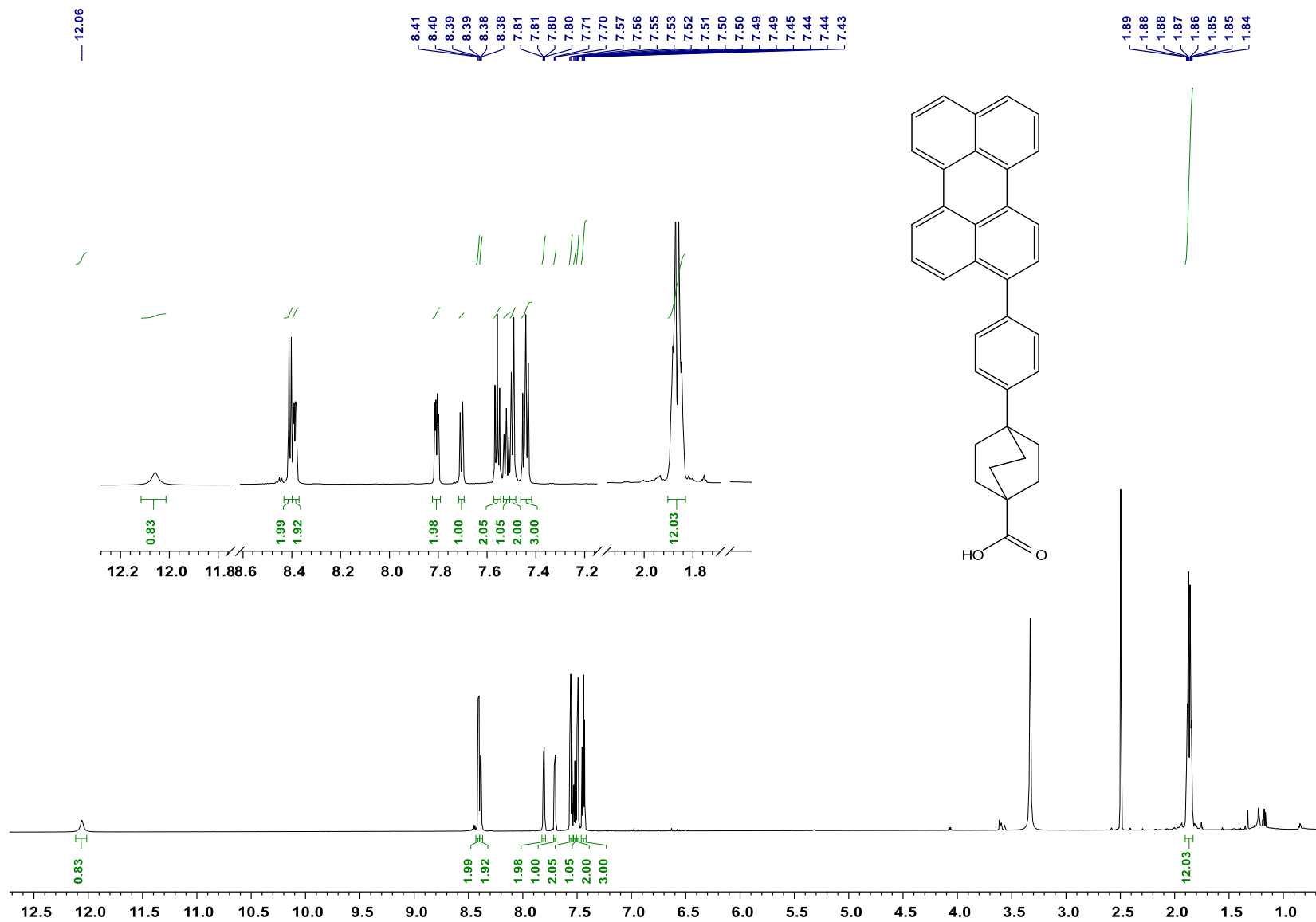


Fig. S16. ¹H NMR (800 MHz, DMSO-d₆), 18.

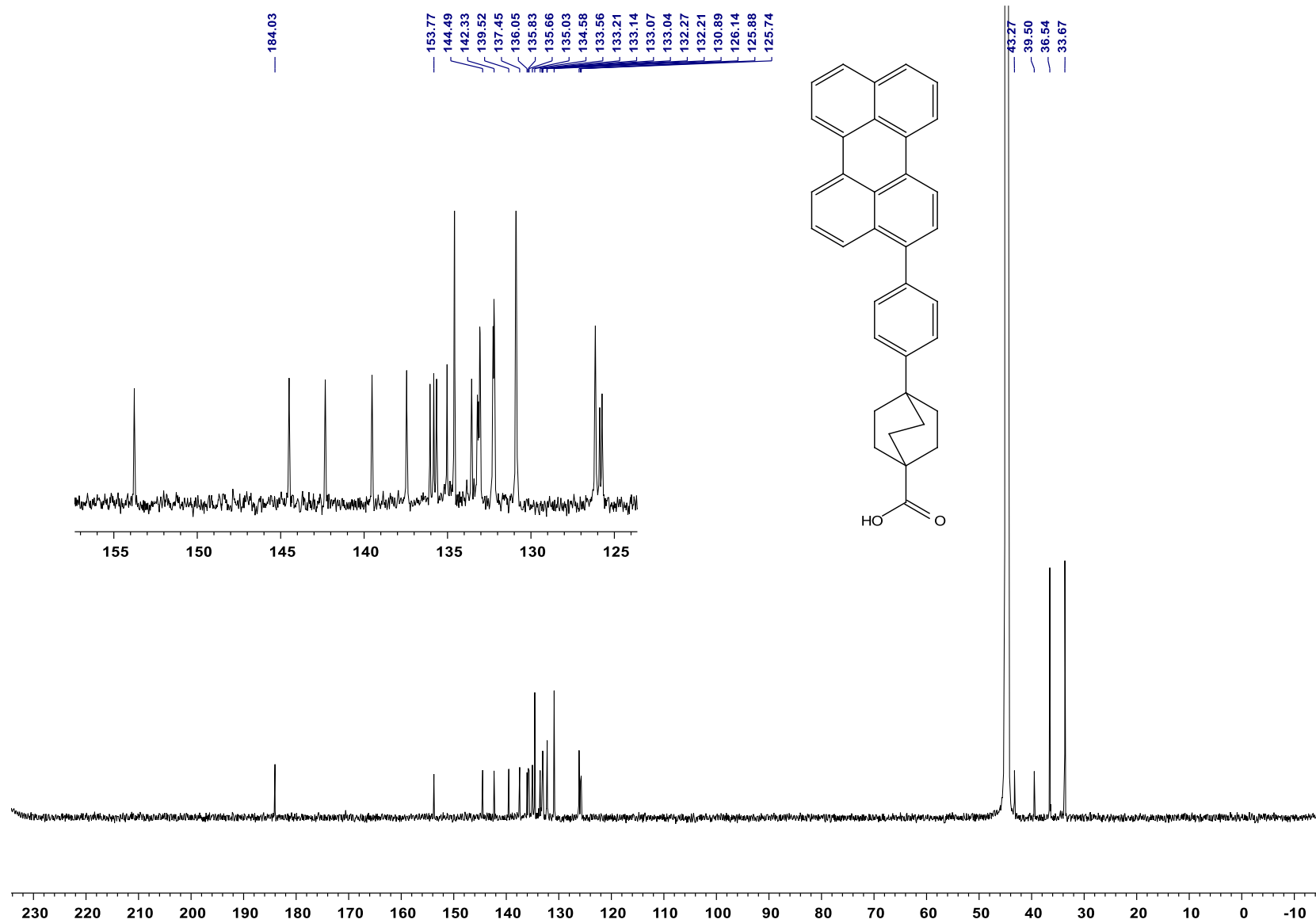


Fig. S17. ^{13}C NMR (201 MHz, DMSO-d_6), 18.

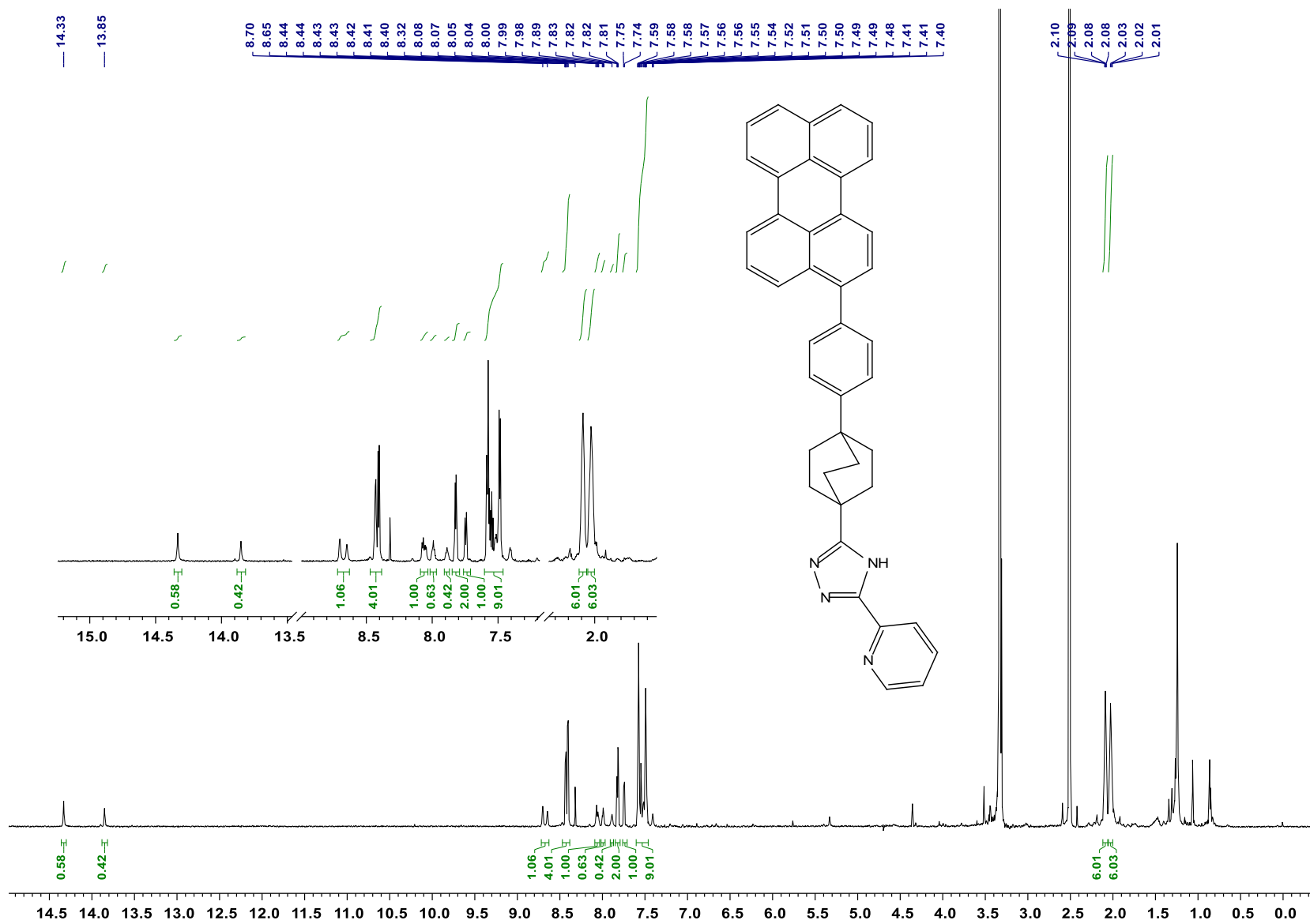


Fig. S18. ¹H NMR (800 MHz, DMSO-d₆), 19.

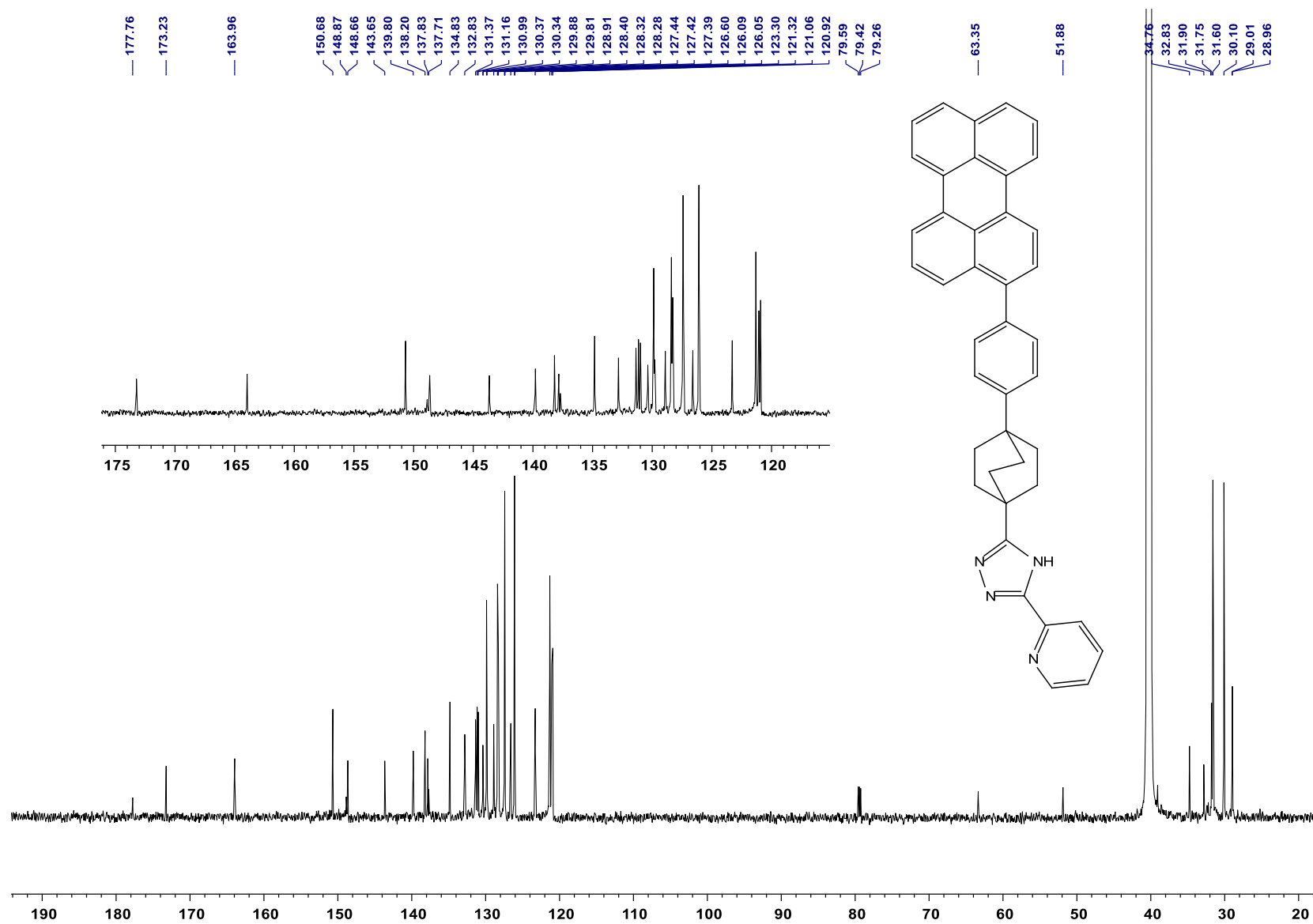


Fig. S19. ^{13}C NMR (201 MHz, DMSO-d_6), 19.

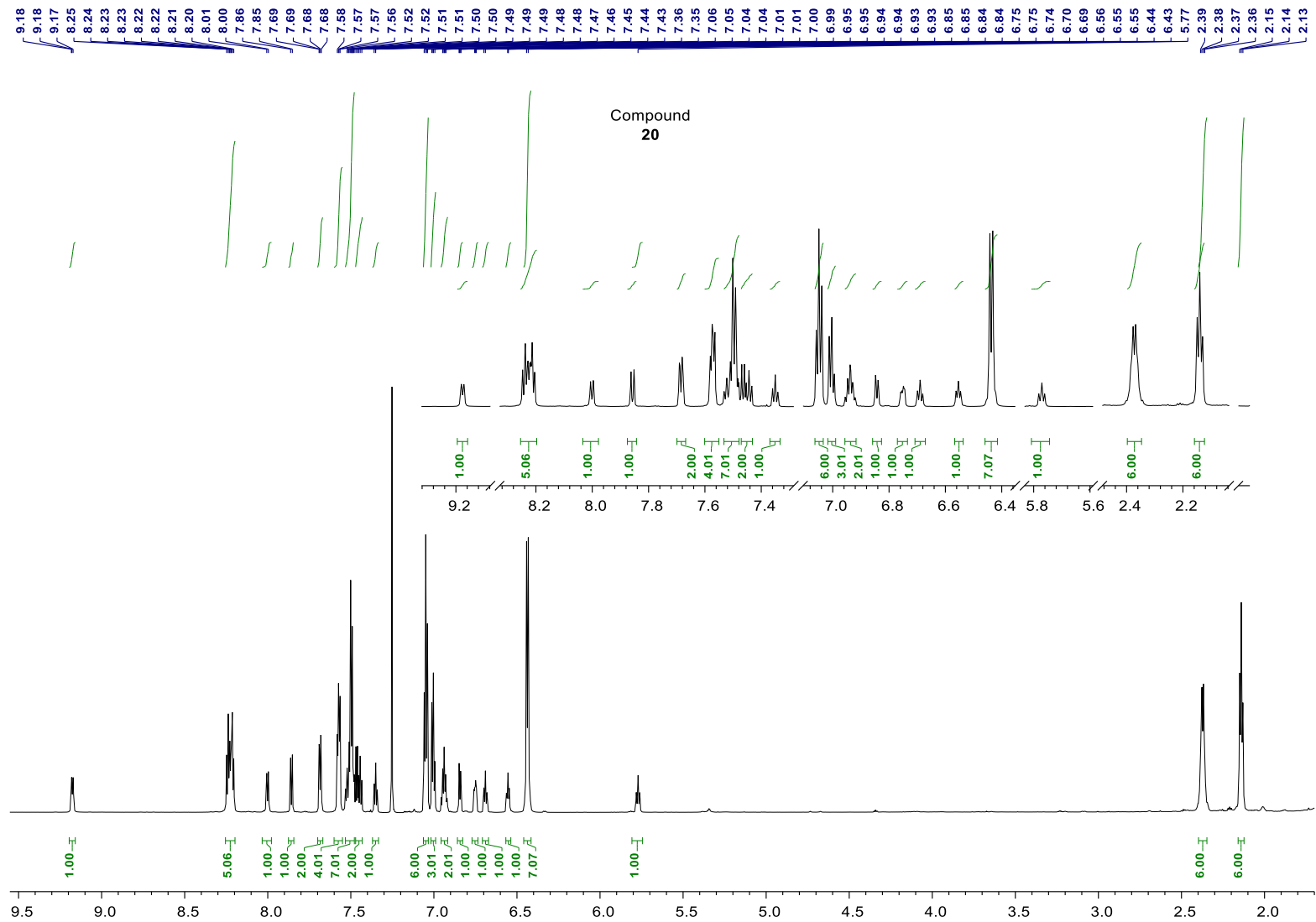


Fig. S20. ¹H NMR (800 MHz, CDCl₃), 20.

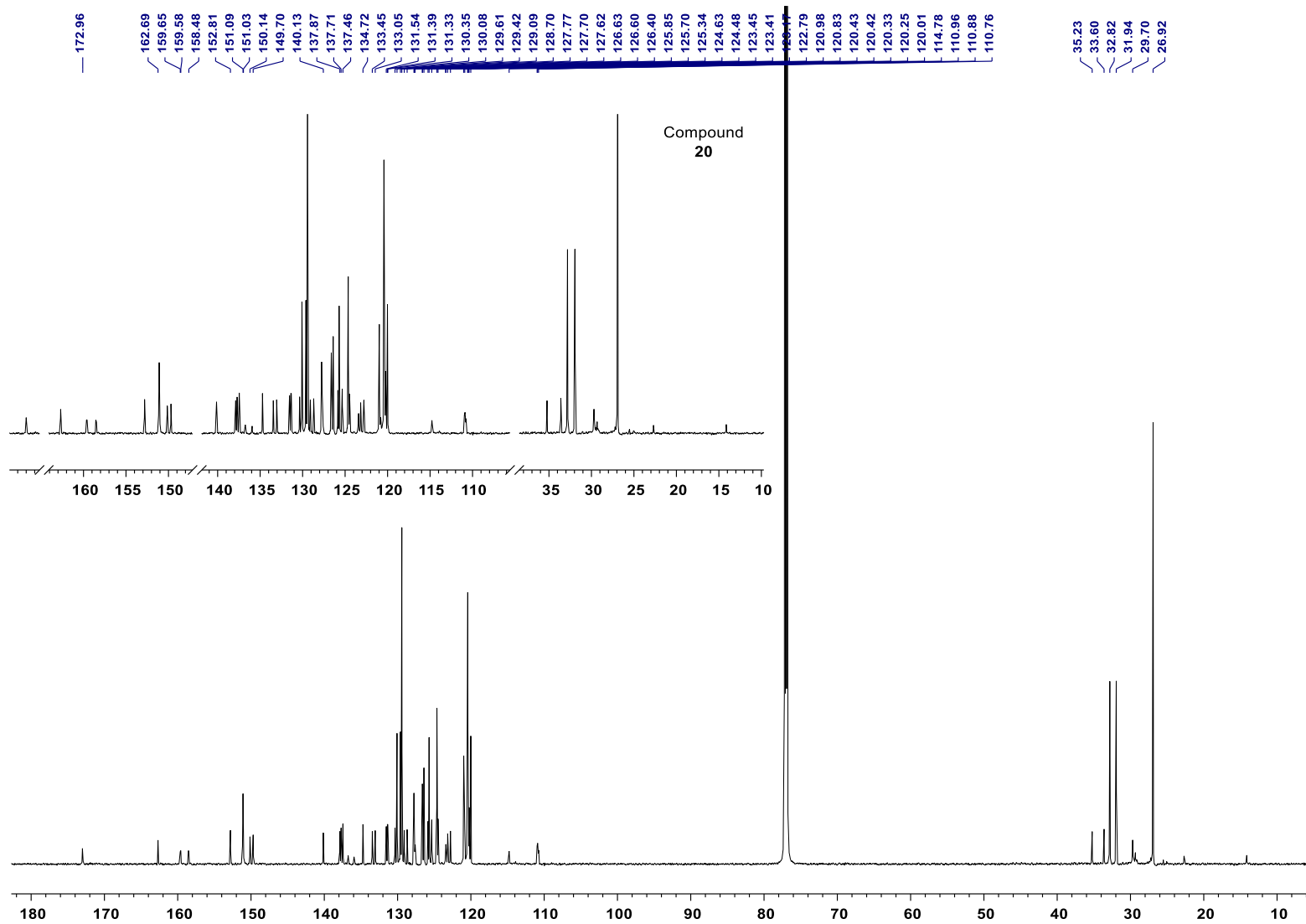


Fig. S21. ^{13}C NMR (201 MHz, CDCl_3), 20.

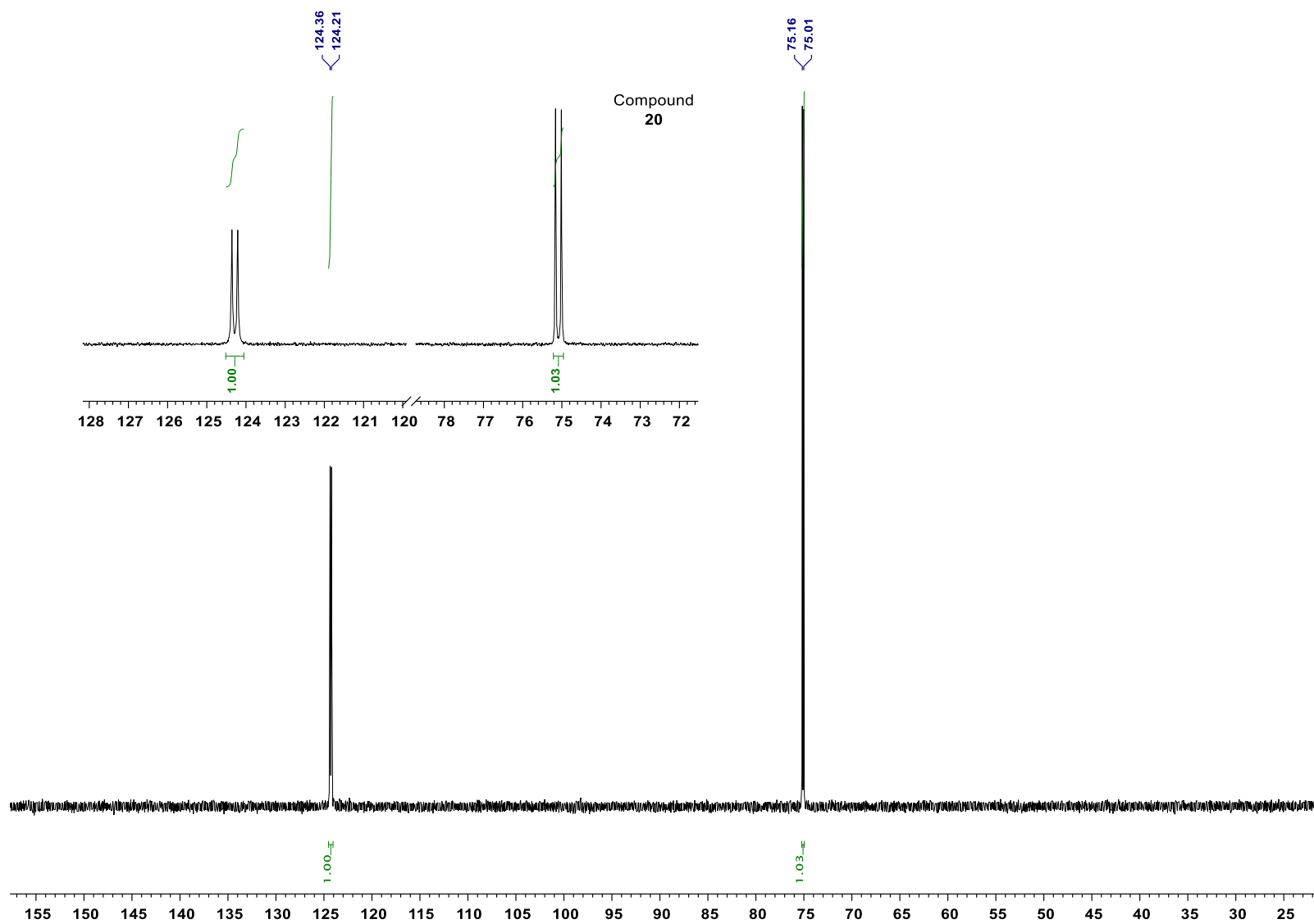


Fig. S22. ^{31}P NMR (162 MHz, CDCl_3), 20.

1. HRMS data

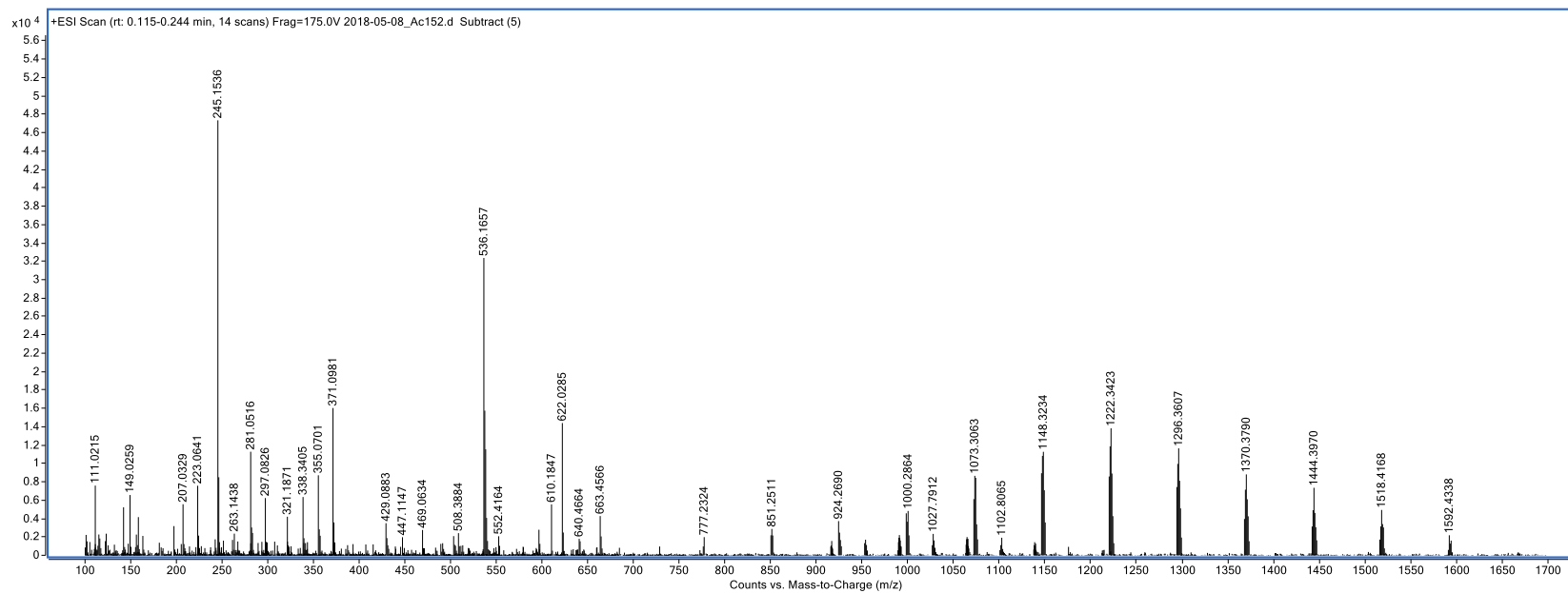


Fig. S23. HRMS (ESI+), 6.

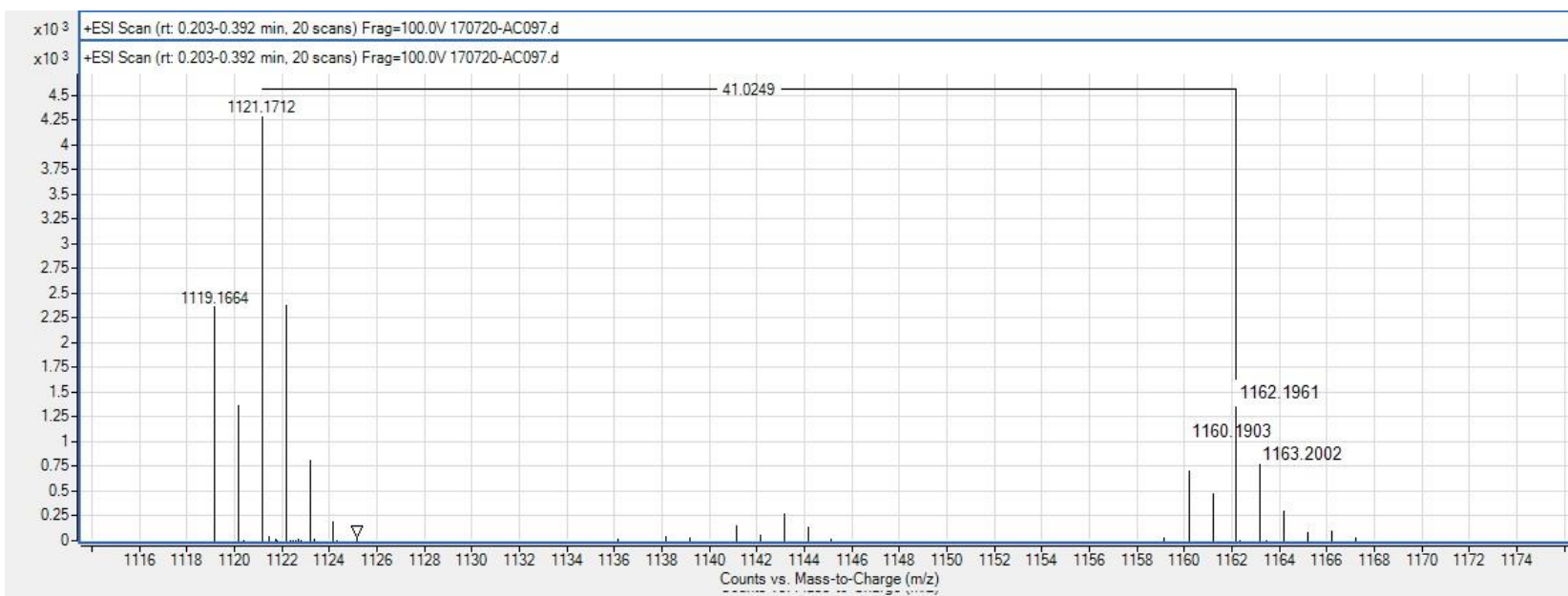


Fig. S24. HRMS (ESI+), 15.

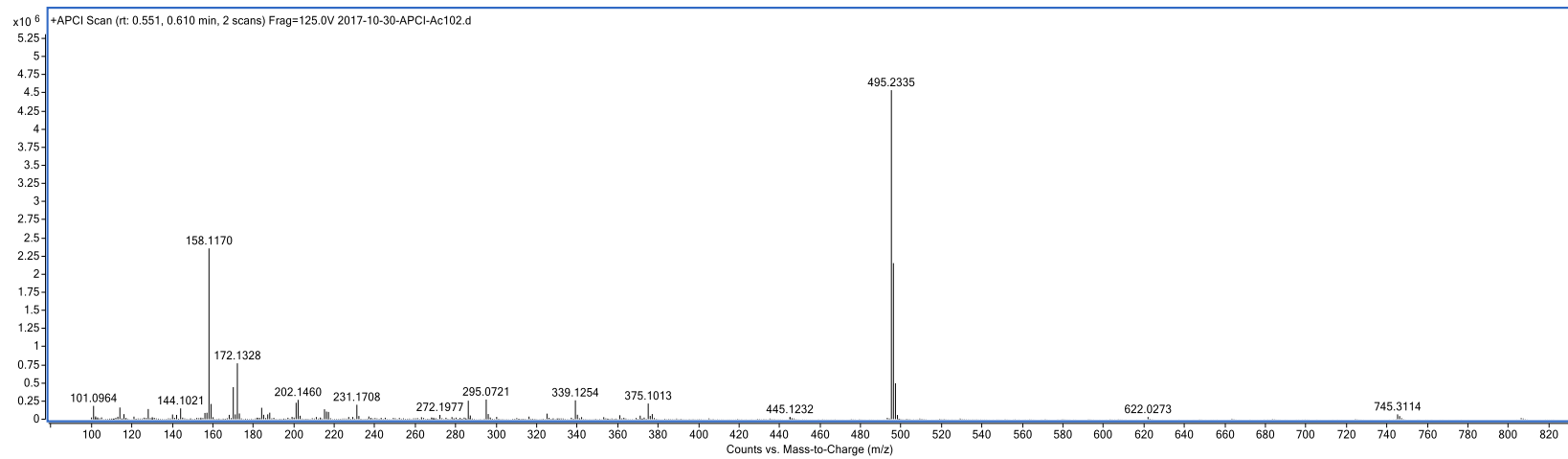


Fig. S25. HRMS (ESI+), 17.

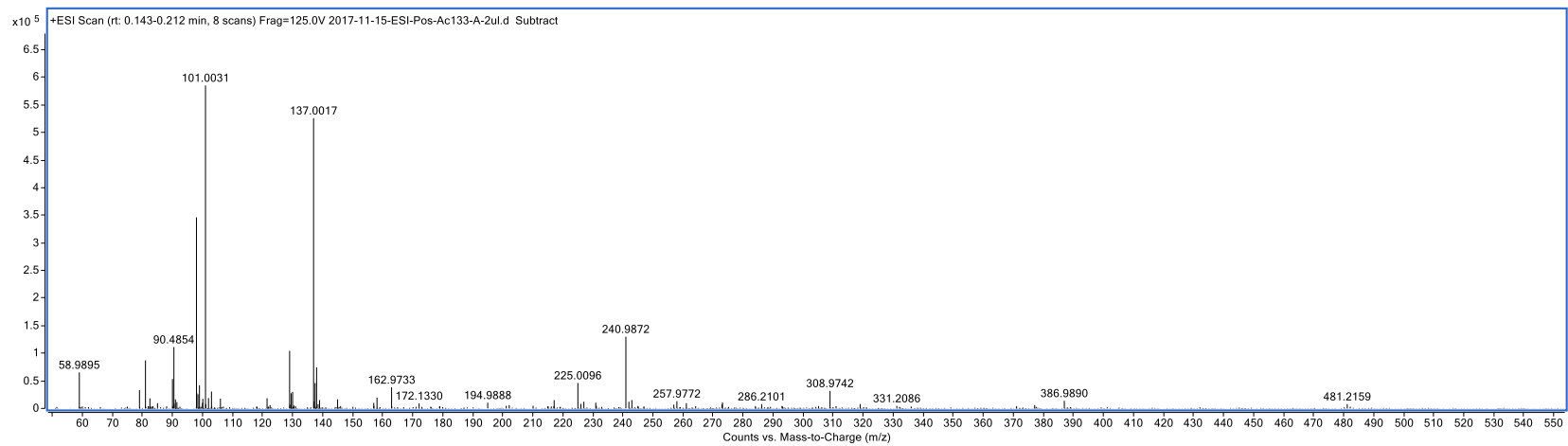


Fig. S26. HRMS (ESI+), 18.

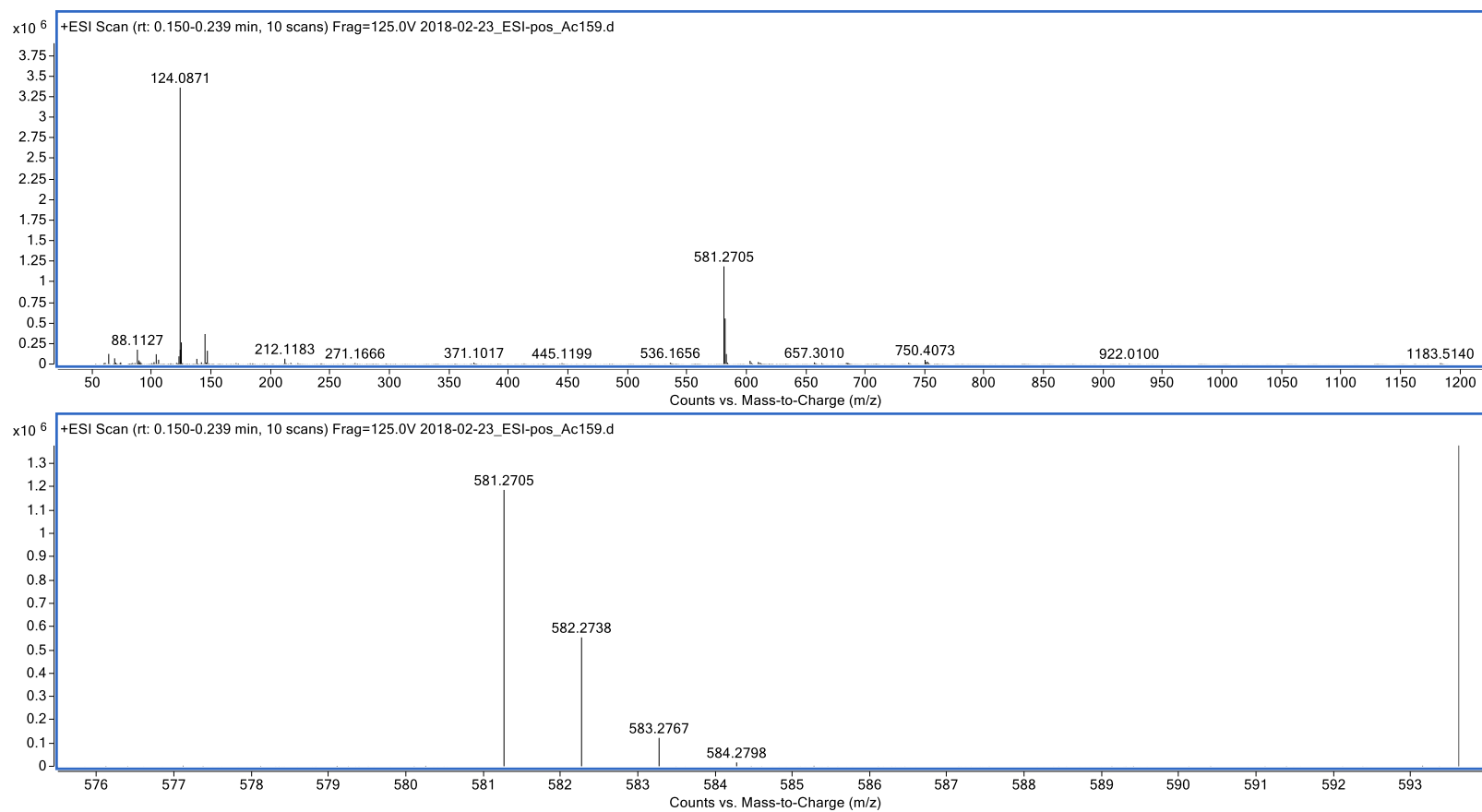


Fig. S27. HRMS (ESI+), 19.

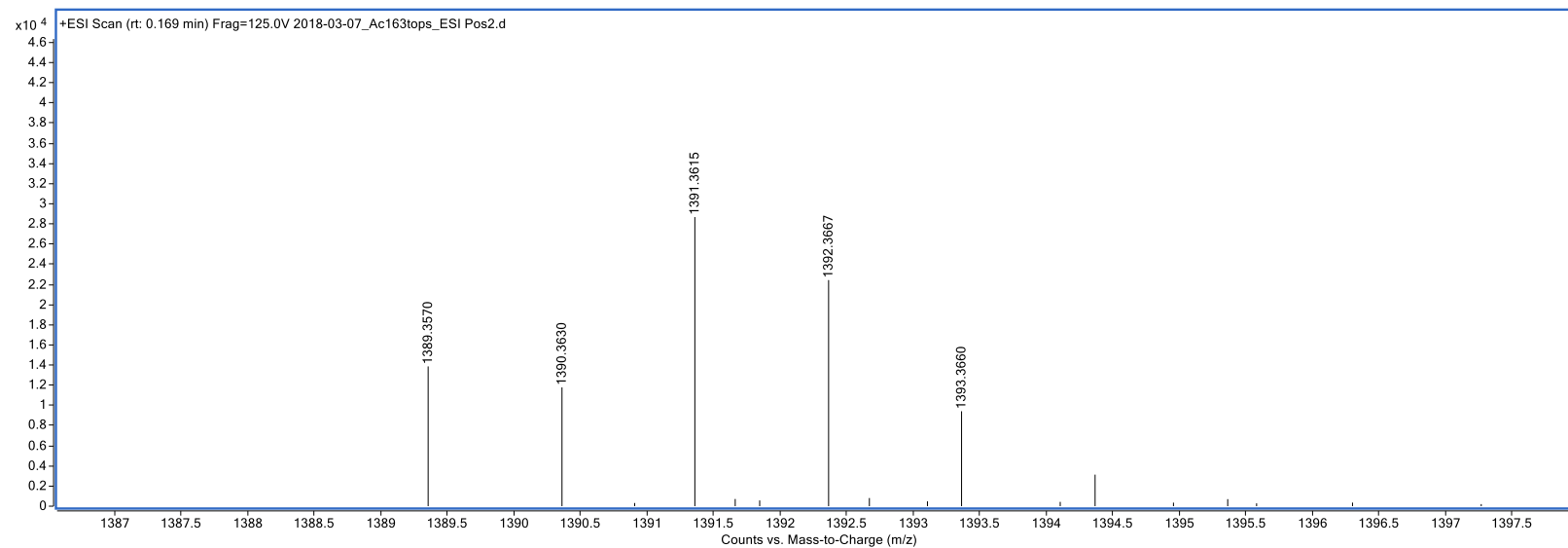
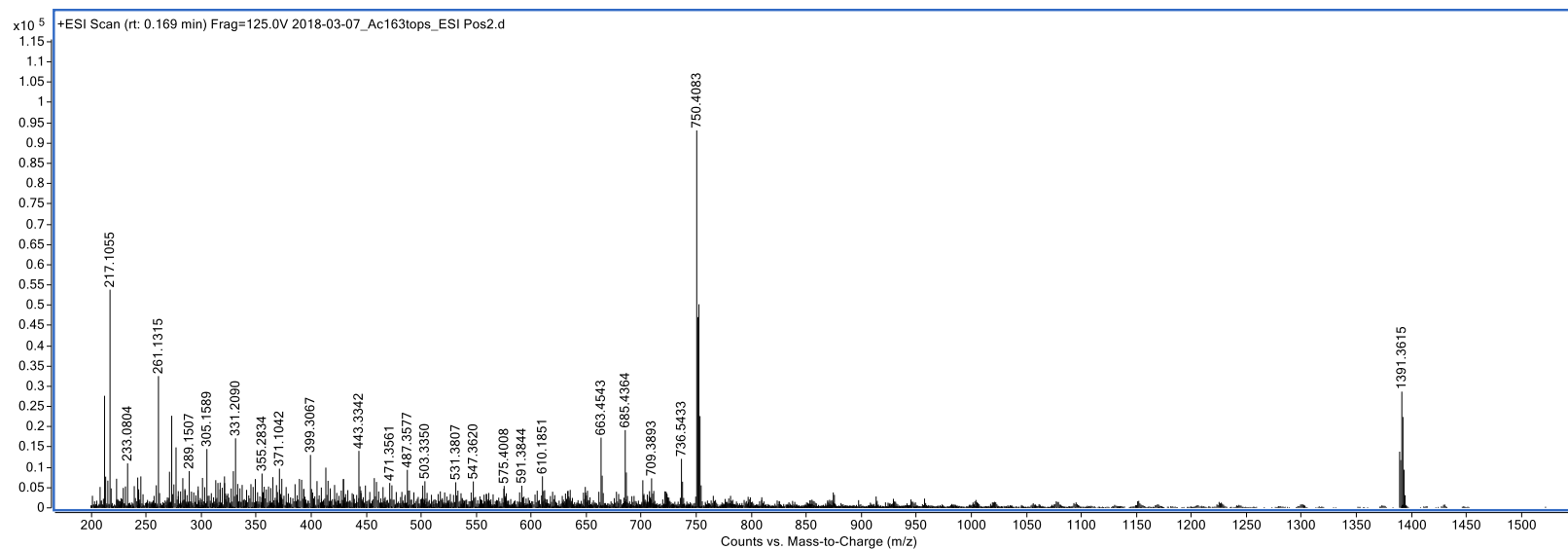


Fig. S28. HRMS (ESI+), 20.